

LOAN COPY: RETURN
AFWL TECHNICAL LIBI
KIRTLAND AFB, N.

0134825



TECH LIBRARY KAFB, NM

Aerodynamic Characteristics at Mach Numbers of 1.5, 1.8, and 2.0 of a Blended Wing-Body Configuration With and Without Integral Canards

A. Warner Robins, Milton Lamb,
and David S. Miller

MAY 1979

NASA





0134825

NASA Technical Paper 1427

Aerodynamic Characteristics at Mach Numbers of 1.5, 1.8, and 2.0 of a Blended Wing-Body Configuration With and Without Integral Canards

A. Warner Robins, Milton Lamb,

and David S. Miller

Langley Research Center

Hampton, Virginia



National Aeronautics
and Space Administration

**Scientific and Technical
Information Office**

1979

SUMMARY

An exploratory, experimental, and theoretical investigation was made of the static longitudinal and lateral aerodynamic characteristics of a cambered, twisted, and blended wing-body configuration with and without integral canard surfaces which were designed to suppress leading-edge vorticity. This investigation was made in the Langley Unitary Plan wind tunnel at Mach numbers of 1.5, 1.8, and 2.0 and at a Reynolds number per meter of 6.56×10^6 .

At the low lift coefficient ($C_L = 0.07$) for which the wing camber surface was designed, both oil-flow and vapor-screen photographs reveal little, if any, upper-surface vortex separation in the very highly swept inboard regions of the wing with or without the canards. Data for the configuration without canards show evidence of significant amounts of leading-edge thrust at lift coefficients at or below the experimental optimum lift coefficient. Under these low lift conditions, any suppression of vortex drag by the canard is outweighed either by the wave and viscous drag contribution of that surface or by the reduction in the upwash which gave rise to leading-edge thrust. The overall results suggest that planform selection is extremely important and that the supplemental application of new calculation techniques should provide a process for the design of supersonic wings in which spanwise distribution of upwash and leading-edge thrust might be rationally controlled and exploited.

INTRODUCTION

Recent interest shown by the U.S. Air Force in supersonic cruise fighter/attack concepts (refs. 1 and 2) has resulted in a NASA program aimed at providing the technology base required for the design of such aircraft. NASA efforts in this program are reported in references 3 to 6 and cover concepts from cruise and maneuver designs in the lower supersonic speed range to those designed for efficient high-speed cruise approaching a Mach number of 3.0. Related efforts of interest are reported in references 7 to 10.

The current investigation had several objectives. The specific purpose was to provide the supersonic concept-development data for a canard-type fighter/attack concept. (See ref. 1.) A general objective was to explore the supersonic aerodynamics of a blended wing-body planform which has regions of very high inboard-leading-edge sweep. Especially examined were the effects of a "no-load" canard on the over-wing flow and on overall configuration efficiency. The no-load canard was designed to suppress the development of the strong discrete vortices associated with such regions of high sweep. Interest in such planforms derives from their lower wing area (and possible lower wing weight) for a given span and lifting length. Both lifting length and span are important to supersonic aerodynamic efficiency. The concept, which has a design Mach number of 1.8, features a deflecting two-dimensional nozzle integrated into inboard trailing-edge flaps. This flap and nozzle combination should provide both high lift and improved low-speed lift-drag ratios. The all-movable canard, which

serves as the longitudinal control surface, is provided with trailing-edge flaps to trim the high lift system in the low-speed regime and, therefore, is a necessary part of the configuration. Thus the purpose, in part, of this investigation was to make the canard a useful component beyond its control role in the supersonic regime.

This investigation was conducted in the Langley Unitary Plan wind tunnel at Mach numbers of 1.5, 1.8, and 2.0 and at a Reynolds number per meter of 6.56×10^6 . Static longitudinal and lateral aerodynamic characteristics are presented, and a qualitative assessment at Mach number 1.8 of both the surface flow and the flow-field characteristics is provided by oil-flow and vapor-screen photographs, respectively. A theoretical correlation is also given.

SYMBOLS

Force and moment data are referred to the body axis system except for lift and drag which are referred to the stability axis system. The moment reference center for the model is located at 46.736 cm from the model nose and 1.377 cm below the horizontal reference line.

b wing reference span, 61.976 cm

\bar{c} wing reference chord, 31.559 cm

C_A axial-force coefficient,
$$\frac{\text{Axial force}}{qS}$$

C_D drag coefficient,
$$\frac{\text{Drag}}{qS}$$

$C_{D,c}$ balance-chamber drag coefficient,
$$\frac{\text{Chamber drag}}{qS}$$

C_L lift coefficient,
$$\frac{\text{Lift}}{qS}$$

$C_{L,\text{opt}}$ optimum lift coefficient for maximum L/D

C_l rolling-moment coefficient,
$$\frac{\text{Rolling moment}}{qSb}$$

$C_{l\beta}$ effective dihedral parameter, per deg

C_m pitching-moment coefficient,
$$\frac{\text{Pitching moment}}{qS\bar{c}}$$

$C_{m,0}$	pitching-moment coefficient at zero lift
C_n	yawing-moment coefficient, $\frac{\text{yawing moment}}{qSb}$
$C_{n\beta}$	directional-stability parameter, per deg
C_p	pressure coefficient
C_y	side-force coefficient, $\frac{\text{Side force}}{qS}$
$C_{y\beta}$	side-force parameter, per deg
L/D	lift-drag ratio
M	free-stream Mach number
q	free-stream dynamic pressure, Pa
S	wing reference area, 1628 cm^2
x	longitudinal station measured from model nose, cm
α	angle of attack, deg
β	angle of sideslip, deg
δ_f	canard flap deflection, positive when trailing edge is down, deg

Model components:

C_C	cambered canard
C_F	flat canard
W	wing

DESCRIPTION OF MODEL

Drawings are shown in figure 1 of the wind-tunnel model and of the canard fighter/attack configuration concept (unofficially designated at Langley as SCIF-2); a photograph of the model in the Langley Unitary Plan wind tunnel is presented as figure 2. The modified arrow wing planform has a continuously curved leading edge out to the 15-percent-semispan station where the wing intersects the canard; the canard is swept back 60° . From 15 percent semispan to 26 percent semispan (the region of the canard root chord), the wing is swept back 79.5° . At 26 percent semispan, the wing leading edge intersects the canard trailing edge; from this point to 46 percent semispan, the wing again has a con-

tinuously curved leading edge. From 46 percent semispan to the tip, the wing is swept back 60° . At the tip, the wing has a slight radius on the leading edge.

The configuration concept on which the model was based (ref. 1) had a design Mach number of 1.8. At that Mach number, the wing camber surface was designed to provide a lift coefficient of 0.07. This value is substantially less than cruise lift coefficient of the airplane configuration, and one which tends to avoid extreme camber shape. Thus, the wing camber surface is that warped plane which, according to the design method of references 11 to 13, would produce the least drag for that planform at that design lift coefficient ($C_L = 0.07$). Unfortunately, this method does not account for the real-flow tendency toward the roll-up of discrete vortices over very highly swept surfaces at moderate and high lift. The canard camber plane was then designed by the same method so that the canard would theoretically have no load at the design lift condition of the wing camber plane. Thus, the flow trailing back from the canard at this condition would be essentially that flow to which the wing was optimized in that region, and the development of discrete vortices over the highly swept portion of the wing should be suppressed.

A range of small deflections of the canard flap was examined to assess the sensitivity of the aerodynamics of the configuration to changes in canard camber-plane geometry and to provide concept-development data. A flat canard (no camber or twist) was tested as well. No attempt was made in the construction of the model to simulate the all-movable canard control. A minimum body was added to the wing to house the balance. (See fig. 1(b).)

The data for the camber and thickness distributions of the configuration without the canards are provided by table I(a) which presents the geometry inputs in the format of references 11 to 13 and of reference 14. Table I(b) provides, in the same format, the thickness ordinates of both the flat canard and the cambered and twisted canard. The camber-plane ordinates of the cambered and twisted canard are also given in table I(b). The portion of the canard surfaces described in table I(b) which would overlap the wing planform of table I(a) is included for lofting purposes only.

TESTS AND INSTRUMENTATION

Tests were conducted in the Langley Unitary Plan wind tunnel at Mach numbers of 1.5, 1.8, and 2.0. The tests were conducted under the following conditions:

Mach number	Stagnation pressure, kPa	Stagnation temperature, K	Reynolds number per meter
1.5	53.2	339	6.56×10^6
1.8	58.5	339	6.56
2.0	63.5	339	6.56

Transition-inducing strips of No. 60 sand grit were applied 1.02 cm behind the leading edges of the airfoil surfaces. The grit size was selected according to the method in reference 15 to insure fully turbulent boundary-layer flow over the model. Forces and moments on the model were measured by means of a six-component strain-gage balance contained within the model. The balance was connected through a supporting sting to the permanent model-actuating system in the wind tunnel. Balance-chamber pressure was measured throughout the test program with a pressure transducer located in the balance cavity and connected to a tube attached to the sting. Balance-chamber drag corrections (corrected to free-stream static pressure) were made to the drag data. Corrections to model angle of attack were made both for tunnel-airflow misalignment and for deflections of the sting and balance under load. Vapor-screen and oil-flow photographs were taken at Mach number 1.8 at selected angles of attack.

PRESENTATION OF RESULTS

The results of the investigation are presented in table II and in the following figures:

	Figure
Longitudinal aerodynamic characteristics	3
Effect on longitudinal aerodynamic characteristics of small variations in flap deflection of cambered canard at $M = 1.8$	4
Oil-flow photographs of configuration without canards at $M = 1.8$	5
Oil-flow photographs of configuration with cambered canards at $M = 1.8$	6
Oil-flow photographs of configuration with flat canards at $M = 1.8$	7
Vapor-screen photographs of configurations without canards at $M = 1.8$	8
Vapor-screen photographs of configuration with cambered canards at $M = 1.8$	9
Vapor-screen photographs of configuration with flat canard at $M = 1.8$	10
Comparison of canard-off and canard-on flow fields and drag at $M = 1.8$	11
Lateral aerodynamic characteristics	12

Experimental and theoretical comparison of longitudinal aerodynamic characteristics of configuration at $M = 1.8$ 13

Comparison of experimental and theoretical values of axial-force coefficient for the configuration without canards at $M = 1.8$ 14

DISCUSSION

Experimental Results

Longitudinal aerodynamic characteristics.— In figure 3, the static longitudinal aerodynamic characteristics of the model without canards are compared with those for the model with either the cambered or the flat canard surface. The configurations with either set of canards have a higher lifting area (and, hence, greater lift-curve slope) than the configuration without canards. In the upwash field of the nose, the flat canard provides higher lift and, hence, higher zero-lift pitching moment $C_{m,0}$ than the cambered (zero-load) canard which produces, as it should, the same pitching moment at design lift as the configuration without canards. When the small lift increments seen in tables II(b) and II(c) (but not discernible in fig. 3) are multiplied by the canard moment arm, they do provide the pitching-moment increments observed in comparing the data in figure 3 for the flat canard with the data for the cambered canard.

The most obvious characteristic in figure 3 is a pitch-up tendency at lift coefficients in the vicinity of 0.25 to 0.35 for all tests. An inspection of the oil-flow photographs of figures 5, 6, and 7 reveals that separated upper-surface flow has already begun in the angle-of-attack range of the pitch break (5° to 6°).

The drag polars show throughout the tests that the model with the canards has higher drag coefficients except at the higher lift coefficients. (See figs. 3 and 4.) The level of maximum lift-drag ratio is higher for the model without the canard. The model with the cambered canard, which was designed so that the flow trailing from it would be identical to the flow for which the wing was shaped, exhibited better performance than the model with the flat canard. In figure 4, which shows the effect at $M = 1.8$ of small variations in the flap deflection of the cambered canard, little distinction can be made in the drag data. If anything, something of the order of 1° upward deflection ($\delta_f = -1$) would appear to provide the best aerodynamic performance, whereas the more positive values of zero-lift pitching moment $C_{m,0}$ provided by a flap deflection of 0° or 0.5° might very well prove best for longitudinal trim at significantly higher levels of stability than shown.

Review of the longitudinal data (figs. 3 and 4), including the oil-flow and vapor-screen photographs of figures 5 to 10, reveals as incorrect the contention which, in part, gave rise to this investigation: the contention that, in the vicinity of design lift (0.07), the vortex-suppression effect of a canard would be required to preclude vortex roll-up over the high-sweep portion of the wing leading edge. Certainly the wing alone is revealed in the oil-flow photograph

of figure 5 to maintain potential flow on the critically sensitive upper surface at design lift ($\alpha = 0^\circ$). Conditions are very different at high lift, however. Figure 11 compares a portion of the flow fields and the associated drag data at $M = 1.8$ for the canard off and canard on (cambered canard). The vapor-screen photographs, in contrast to previous such photographs, were taken from outside the test-section window with the fan of light at model station 40.64 (well aft of the canard station). Immediately apparent are the pair of very strong vortices with the canard off at an angle of attack of 12° . The corresponding photograph with the canard on shows only some lower grade vorticity and surface separation in addition to the canard-tip vortices and the shock field from the loaded canard. Obviously, the additional viscous and wave drag of the canard provides a drag increment at low lift. At high lift, however, the greater lifting area of the canard and its effect in improving the flow over the wing results in a significant drag decrement.

Lateral-directional characteristics.— The basic sideslip data, which were taken nominally at $\beta = -4^\circ$ to 10° for the three basic configurations, were very linear and, hence, are not shown. These data can be essentially generated from the sideslip derivatives shown as a function of angle of attack in figure 12. Very little difference is seen in lateral characteristics except that the canards improve the wing upper-surface flow and, consequently, improve linearity in effective dihedral. Directional stability is not seen to degrade with or without canards throughout the range of lift coefficients tested. This is most likely the effect of the airfoil-like, forebody cross section advancing into the subsonic cross flow much as an autogiro blade would. (See ref. 16.)

Experimental and Theoretical Comparisons

Experimental and theoretical comparisons at the design Mach number of 1.8 for the model without a canard and with the flat canard are presented in figure 13. Zero-lift wave drag and drag due to lift were calculated by the method of references 11 to 13 for no limit and for a limit of three-quarters of a vacuum in pressure coefficient. Viscous drag was calculated by the method of reference 17. The configuration with the flat canard is selected for comparison since the method of references 11 to 13 does not yet permit consideration of a cambered and/or twisted auxiliary horizontal surface.

An especially interesting result is seen in figure 13 in the comparisons of C_m and α plotted against C_L for the model with canards and without canards. The theoretical curve for no pressure limit (where pressure could be less than vacuum) does not exhibit breaks in linearity; however, the theoretical curves for limited pressure do exhibit breaks in linearity, and the experimental data do also. The breaks in linearity are more pronounced for theory than for experiment, since the theory does not account for any lift induced by the development of vortices over the wing that were previously noted and are described in reference 18. Thus, the theory without limited pressure (the theory used for the design of the wing) produces a shape which, in the vicinity of a lift coefficient of 0.3, begins to require potential-flow pressures on the upper surface which are physically impossible to achieve. When consideration is given analytically (ref. 18) to the vortex-interference lift, which replaces the potential

flow apparently no longer possible over the upper surface of the configuration without canard, theory better represents experiment both qualitatively and quantitatively.

Regarding drag, predictions (refs. 11 to 13) for the model without canards appear to be slightly high (0.00044) near zero lift. The striking characteristic for this configuration, however, is the improved drag-polar shape and the significantly higher experimental lift-drag ratios in the range of optimum lift coefficient $C_{L, \text{opt}}$. The wing camber shape was designed for a lift coefficient of about 0.07 by a theory which assumes no leading-edge thrust at that point, and the experimental $C_{L, \text{opt}}$ occurs at 0.18, well past (approximately 2.5°) the design attitude of 0° angle of attack. Consequently, the upwash must have increased well beyond that for which the surface was designed and must have produced leading-edge thrust (particularly inboard where the wing leading edge is blunt and where it follows the high-sweep portion of the leading edge).

The addition of the canard is seen to have significantly degraded the lift-drag ratio near $C_{L, \text{opt}}$ (fig. 13), suggesting that such a surface would significantly reduce the upwash and consequent thrust of the inboard portions of the wing downstream of the canard trailing edge. The fact, as previously noted, that a slightly upward deflection of the canard flap ($\delta_f = -1^\circ$) improved the experimental aerodynamic performance while permitting increased upwash on the wing leading edge, would further support this view.

To more directly explore the extent of leading-edge thrust of the canard-off configuration, the calculations shown in figure 14 were made. Using the methods of references 11 to 13 and 19, theoretical axial-force coefficients were calculated for both no leading-edge thrust and full leading-edge thrust. The experimental values shown were adjusted by the small increment in drag (0.00044) previously noted, so that the theoretical and experimental values would be coincident at the lift coefficient (0.07) for which the wing camber surface was designed. The two oil-flow photographs taken at design camber attitude ($\alpha = 0^\circ$) and at $\alpha = 4^\circ$ ($C_L = 0.28$) are repeated in this figure to show the clean upper-surface flow and the very nonpotential flow, respectively, for those two relevant conditions. Immediately apparent is the indication of experimental, full leading-edge thrust at experimental optimum lift $C_{L, \text{opt}}$. Also apparent is the rapid loss in percent of leading-edge thrust as lift is further increased to and beyond the lift coefficient (0.28) corresponding to the photograph (fig. 14) showing substantial upper-surface flow breakdown.

Evidently, this wing planform, which has a high upwash region of its leading edge inboard where the leading edge is relatively blunt, can, indeed, achieve significant levels of leading-edge thrust at supersonic speeds where more conventional thin wings with straight, subsonic leading edges and highest upwash at the tip cannot achieve leading-edge thrust. This fact would suggest that planform selection is extremely important, and, further, that use of the method of reference 19 in conjunction with that of references 11 to 13 should permit the design of supersonic wings in which spanwise distribution of upwash or leading-edge thrust might be rationally controlled and exploited.

CONCLUDING REMARKS

An exploratory investigation was made of both theoretical and experimental static longitudinal and lateral aerodynamic characteristics of a cambered, twisted, and blended wing-body concept. The wing-body was investigated with and without integral canard surfaces designed to suppress leading-edge vorticity. This investigation was conducted in the Langley Unitary Plan wind tunnel at Mach numbers of 1.5, 1.8, and 2.0 and at a Reynolds number per meter of 6.56×10^6 .

At the low lift coefficient ($C_L = 0.07$) for which the wing camber surface was designed, both oil-flow and vapor-screen photographs reveal little, if any, upper-surface vortex separation in the very highly swept inboard regions of the wing with or without the canard surface. Data for the configuration without canards show evidence of significant amounts of leading-edge thrust at lift coefficients at or below the experimental optimum lift coefficient. Under these low lift conditions, any suppression of vortex drag by the canard is outweighed either by the wave and viscous drag contribution of that surface or by the reduction in the upwash which gave rise to leading-edge thrust. The overall results suggest that planform selection is extremely important and that the supplemental application of new calculation techniques should provide a process for the design of supersonic wings in which spanwise distribution of upwash and leading-edge thrust might be rationally controlled and exploited.

Langley Research Center
National Aeronautics and Space Administration
Hampton, VA 23665
March 21, 1979

REFERENCES

1. Shrout, Barrett L.; Morris, Odell A.; Robins, A. Warner; and Dollyhigh, Samuel M.: Review of NASA Supercruise Configuration Studies. Design Conference Proceedings - Technology for Supersonic Cruise Military Aircraft, Volume I, AFFDL-TR-77-85, Vol. I, U.S. Air Force, 1976.
2. Dollyhigh, Samuel M.; Ayers, Theodore G.; Morris, Odell A.; and Miller, David M.: Designing for Supercruise and Maneuver. Design Conference Proceedings - Technology for Supersonic Cruise Military Aircraft, Volume I, AFFDL-TR-77-85, Vol. I, U.S. Air Force, 1976.
3. Dollyhigh, Samuel M.: Subsonic and Supersonic Longitudinal Stability and Control Characteristics of an Aft-Tail Fighter Configuration With Cambered and Uncambered Wings and Cambered Fuselage. NASA TN D-8472, 1977.
4. Shrout, Barrett L.: Aerodynamic Characteristics at Mach Numbers From 0.6 to 2.16 of a Supersonic Cruise Fighter Configuration With a Design Mach Number of 1.8. NASA TM X-3559, 1977.
5. Morris, Odell A.: Subsonic and Supersonic Aerodynamic Characteristics of a Supersonic Cruise Fighter Model With a Twisted and Cambered Wing With 74° Sweep. NASA TM X-3530, 1977.
6. Dollyhigh, Samuel M.: Experimental Aerodynamic Characteristics at Mach Numbers From 0.60 to 2.70 of Two Supersonic Cruise Fighter Configurations. NASA TM-78764, 1979.
7. Dollyhigh, Samuel M.; Morris, Odell A.; and Adams, Mary S.: Experimental Effects of Fuselage Camber on Longitudinal Aerodynamic Characteristics of a Series of Wing-Fuselage Configurations at a Mach Number of 1.41. NASA TM X-3411, 1976.
8. Dollyhigh, Samuel M.: Wing-Camber Effects on Longitudinal Aerodynamic Characteristics of a Variable-Sweep Fighter Configuration at Mach Numbers From 1.60 to 2.86. NASA TM X-2826, 1973.
9. Dollyhigh, Samuel M.; Monta, William J.; and Sangiorgio, Giuliana: Longitudinal Aerodynamic Characteristics at Mach 0.60 to 2.86 of a Fighter Configuration With Strut Braced Wing. NASA TP-1102, 1977.
10. Dollyhigh, Samuel M.; Sangiorgio, Giuliana; and Monta, William J.: Effects of Stores on Longitudinal Aerodynamic Characteristics of a Fighter at Supersonic Speeds. NASA TP-1175, 1978.
11. Middleton, W. D.; and Lundry, J. L.: A Computational System for Aerodynamic Design and Analysis of Supersonic Aircraft. Part 1 - General Description and Theoretical Development. NASA CR-2715, 1976.

12. Middleton, W. D.; Lundry, J. L.; and Coleman, R. G.: A Computational System for Aerodynamic Design and Analysis of Supersonic Aircraft. Part 2 - User's Manual. NASA CR-2716, 1976.
13. Middleton, W. D.; Lundry, J. L.; and Coleman, R. G.: A Computational System for Aerodynamic Design and Analysis of Supersonic Aircraft. Part 3 - Computer Program Description. NASA CR-2717, 1976.
14. Craidon, Charlotte B.: Description of a Digital Computer Program for Airplane Configuration Plots. NASA TM X-2074, 1970.
15. Braslow, Albert L.; Hicks, Raymond M.; and Harris, Roy V., Jr.: Use of Grit-Type Boundary-Layer-Transition Trips on Wind-Tunnel Models. Conference on Aircraft Aerodynamics, NASA SP-124, 1966, pp. 19-36. (Also available as NASA TN D-3579.)
16. Polhamus, Edward C.; Geller, Edward W.; and Grunwald, Kalman J.: Pressure and Force Characteristics of Noncircular Cylinders as Affected by Reynolds Number With a Method Included for Determining the Potential Flow About Arbitrary Shapes. NASA TR R-46, 1959.
17. Sommer, Simon C.; and Short, Barbara J.: Free-Flight Measurements of Turbulent-Boundary-Layer Skin Friction in the Presence of Severe Aerodynamic Heating at Mach Numbers From 2.8 to 7.0. NACA TN 3391, 1955.
18. Polhamus, Edward C.: Predictions of Vortex-Lift Characteristics by a Leading-Edge Suction Analogy. J. Aircr., vol. 8, no. 4, Apr. 1971, pp. 193-199.
19. Carlson, Harry W.; and Mack, Robert J.: Estimation of Leading-Edge Thrust for Supersonic Wings of Arbitrary Planform. NASA TP-1270, 1978.



TABLE I.- INPUT GEOMETRIC CHARACTERISTICS OF WIND-TUNNEL MODEL IN CENTIMETERS

(a) Model without canards

1628.07												REF A
0.0	.500	.750	1.250	2.500	5.000	7.500	10.000	15.000	20.000	XAF	10	
25.000	30.000	35.000	40.000	45.000	50.000	55.000	60.000	65.000	70.000	XAF	20	
75.000	80.000	85.000	90.000	95.000	100.000					XAF	26	
0.000	0.000	2.134	68.580							WORG	1	
.447	1.031	2.062	67.925							WORG	2	
1.565	2.068	1.849	66.604							WORG	3	
3.190	3.099	1.504	64.770							WORG	4	
5.720	4.130	.813	62.032							WORG	5	
10.119	5.166	.020	57.429							WORG	6	
21.234	7.229	0.000	45.898							WORG	8	
26.060	8.265	-.046	40.869							WORG	9	
32.756	10.328	-.279	33.757							WORG	11	
35.662	11.364	-.381	30.648							WORG	12	
38.303	12.395	-.475	27.798							WORG	13	
40.681	13.426	-.559	25.944							WORG	14	
44.618	15.494	-.696	23.658							WORG	16	
49.982	18.593	-.884	20.772							WORG	19	
55.352	21.692	-1.072	17.882							WORG	22	
60.719	24.790	-1.260	14.994							WORG	25	
66.086	27.889	-1.448	12.106							WORG	28	
67.869	28.920	-1.509	11.151							WORG	29	
70.063	29.957	-1.588	9.779							WORG	30	
76.200	30.988	-1.803	4.470							WORG	31	
0.000	-.015	-.025	-.038	-.076	-.173	-.279	-.401	-.648	-.914	TZORD	1	
-1.199	-1.488	-1.786	-2.083	-2.375	-2.662	-2.939	-3.198	-3.439	-3.663	TZORD	1	
-3.856	-4.023	-4.161	-4.265	-4.333	-4.369					TZORD	1	
0.000	-.020	-.030	-.048	-.099	-.198	-.320	-.437	-.699	-.973	TZORD	2	
-1.265	-1.560	-1.859	-2.159	-2.449	-2.733	-3.002	-3.256	-3.490	-3.698	TZORD	2	
-3.879	-4.031	-4.150	-4.237	-4.288	-4.298					TZORD	2	
0.000	-.013	-.018	-.028	-.069	-.157	-.264	-.376	-.625	-.894	TZORD	3	
-1.173	-1.468	-1.781	-2.055	-2.339	-2.637	-2.880	-3.124	-3.348	-3.548	TZORD	3	
-3.719	-3.861	-3.970	-4.046	-4.084	-4.084					TZORD	3	
0.000	-.005	-.008	-.014	-.038	-.091	-.175	-.267	-.492	-.742	TZORD	4	
-1.016	-1.294	-1.568	-1.839	-2.111	-2.367	-2.598	-2.831	-3.033	-3.185	TZORD	4	
-3.322	-3.419	-3.500	-3.561	-3.581	-3.571					TZORD	4	
0.000	.008	.013	.023	.046	.056	.036	-.020	-.152	-.330	TZORD	5	
-.572	-.810	-1.052	-1.285	-1.514	-1.735	-1.941	-2.123	-2.281	-2.418	TZORD	5	
-2.527	-2.606	-2.654	-2.670	-2.649	-2.596					TZORD	5	

TABLE I.- Continued

(a) Continued

0.000	.030	.046	.076	.147	.257	.318	.345	.320	.206	TZORD	6
.046	-.137	-.328	-.508	-.681	-.848	-1.006	-1.153	-1.288	-1.407	TZORD	6
-1.509	-1.590	-1.648	-1.687	-1.699	-1.689					TZORD	6
0.000	.025	.036	.056	.117	.224	.310	.358	.376	.356	TZORD	8
.300	.229	.135	.028	-.086	-.208	-.335	-.472	-.607	-.747	TZORD	8
-.889	-1.029	-1.168	-1.308	-1.445	-1.582					TZORD	8
0.000	.018	.025	.046	.086	.165	.229	.257	.279	.279	TZORD	9
.249	.203	.142	.066	-.015	-.074	-.218	-.328	-.445	-.566	TZORD	9
-.696	-.828	-.960	-1.100	-1.237	-1.382					TZORD	9
0.000	.013	.018	.030	.061	.117	.168	.188	.221	.234	TZORD	11
.229	.218	.193	.157	.117	.071	.020	-.036	-.094	-.157	TZORD	11
-.226	-.292	-.363	-.439	-.513	-.592					TZORD	11
0.000	.010	.015	.025	.056	.102	.145	.178	.216	.239	TZORD	12
.249	.249	.244	.231	.213	.191	.165	.132	.097	.058	TZORD	12
.020	-.023	-.066	-.114	-.163	-.211					TZORD	12
0.000	.010	.015	.023	.046	.091	.122	.147	.185	.211	TZORD	13
.229	.239	.241	.241	.236	.229	.216	.198	.183	.160	TZORD	13
.137	.114	.086	.061	.030	0.000					TZORD	13
0.000	.005	.010	.018	.036	.066	.007	.124	.157	.183	TZORD	14
.198	.208	.216	.218	.216	.211	.203	.193	.180	.168	TZORD	14
.152	.135	.114	.094	.071	.048					TZORD	14
0.000	.005	.005	.010	.023	.043	.058	.074	.097	.112	TZORD	16
.122	.127	.132	.132	.130	.124	.117	.109	.099	.089	TZORD	16
.076	.061	.046	.030	.013	-.005					TZORD	16
0.000	.003	.005	.005	.013	.023	.033	.046	.056	.066	TZORD	19
.069	.069	.066	.061	.053	.046	.036	.025	.015		TZORD	19
.005	-.010	-.023	-.036	-.051	-.066					TZORD	19
0.000	.003	.003	.005	.010	.018	.028	.036	.046	.053	TZORD	22
.056	.056	.056	.056	.053	.046	.043	.036	.028	.020	TZORD	22
.013	.005	-.005	-.015	-.025	-.036					TZORD	22
0.000	.003	.003	.005	.008	.015	.020	.025	.036	.043	TZORD	25
.046	.048	.051	.051	.048	.046	.041	.038	.033	.043	TZORD	25
.028	.023	.018	.010	.005	-.003					TZORD	25
0.000	.003	.003	.003	.005	.013	.015	.023	.036	.041	TZORD	28
.046	.051	.053	.056	.056	.056	.056	.053	.053	.051	TZORD	28
.046	.046	.041	.036	.030	.025					TZORD	28
0.000	.003	.003	.003	.005	.013	.015	.023	.033	.038	TZORD	29
.042	.046	.048	.051	.051	.051	.051	.046	.046	.041	TZORD	29
.036	.030	.025	.015	.010	0.000					TZORD	29

TABLE I.- Continued

(a) Continued

0.000	.003	.003	.003	.005	.010	.015	.023	.033	.036	TZORD	30
.043	.046	.048	.051	.051	.051	.048	.046	.043	.038	TZORD	30
.036	.030	.023	.015	.010	0.000					TZORD	30
0.000	0.000	0.000	.003	.003	.005	.008	.010	.015	.023	TZORD	31
.025	.033	.032	.043	.048	.053	.058	.066	.069	.076	TZORD	31
.081	.086	.091	.097	.102	.107					TZORD	31
0.0	.304	.368	.469	.647	.875	1.059	1.213	1.459	1.645	WAFORD	1
1.788	1.892	1.962	1.997	1.996	1.954	1.868	1.743	1.586	1.402	WAFORD	1
1.195	.967	.729	.490	.250	.009					WAFORD	1
0.0	.304	.368	.469	.647	.875	1.059	1.213	1.459	1.645	WAFORD	2
1.788	1.892	1.962	1.997	1.996	1.954	1.868	1.743	1.586	1.402	WAFORD	2
1.195	.967	.729	.490	.250	.009					WAFORD	2
0.0	.304	.368	.469	.647	.875	1.059	1.213	1.459	1.645	WAFORD	3
1.788	1.892	1.962	1.997	1.996	1.954	1.868	1.743	1.586	1.402	WAFORD	3
1.195	.967	.729	.490	.250	.009					WAFORD	3
0.0	.304	.368	.469	.647	.875	1.059	1.213	1.459	1.645	WAFORD	4
1.788	1.892	1.962	1.997	1.996	1.954	1.868	1.743	1.586	1.402	WAFORD	4
1.195	.967	.729	.490	.250	.009					WAFORD	4
0.0	.304	.368	.469	.647	.875	1.059	1.213	1.459	1.645	WAFORD	5
1.788	1.892	1.962	1.997	1.996	1.954	1.868	1.743	1.586	1.402	WAFORD	5
1.195	.967	.729	.490	.250	.009					WAFORD	5
0.0	.304	.368	.469	.647	.875	1.059	1.213	1.459	1.645	WAFORD	6
1.788	1.892	1.962	1.997	1.996	1.954	1.868	1.743	1.586	1.402	WAFORD	6
1.195	.967	.729	.490	.250	.009					WAFORD	6
0.0	.304	.368	.469	.647	.875	1.059	1.213	1.459	1.645	WAFORD	8
1.788	1.892	1.962	1.997	1.996	1.954	1.868	1.743	1.586	1.402	WAFORD	8
1.195	.967	.729	.490	.250	.009					WAFORD	8
0.0	.304	.368	.469	.647	.875	1.059	1.213	1.459	1.645	WAFORD	9
1.788	1.892	1.962	1.997	1.996	1.954	1.868	1.743	1.586	1.402	WAFORD	9
1.195	.967	.729	.490	.250	.009					WAFORD	9
0.0	.304	.368	.469	.647	.875	1.059	1.213	1.459	1.645	WAFORD	11
1.788	1.892	1.962	1.997	1.996	1.954	1.868	1.743	1.586	1.402	WAFORD	11
1.195	.967	.729	.490	.250	.009					WAFORD	11
0.0	.304	.368	.469	.647	.875	1.059	1.213	1.459	1.645	WAFORD	12
1.788	1.892	1.962	1.997	1.996	1.954	1.868	1.743	1.586	1.402	WAFORD	12
1.195	.967	.729	.490	.250	.009					WAFORD	12

TABLE I.- Continued

(a) Concluded

0.0	.304	.368	.469	.647	.875	1.059	1.213	1.459	1.645	WAFORD13
1.788	1.892	1.962	1.997	1.996	1.954	1.868	1.743	1.586	1.402	WAFORD13
1.195	.967	.729	.490	.250	.009					WAFORD13
0.0	.304	.368	.469	.647	.875	1.059	1.213	1.459	1.645	WAFORD14
1.788	1.892	1.962	1.997	1.996	1.954	1.868	1.743	1.586	1.402	WAFORD14
1.195	.967	.729	.490	.250	.009					WAFORD14
0.0	.304	.368	.469	.647	.875	1.059	1.213	1.459	1.645	WAFORD16
1.788	1.892	1.962	1.997	1.996	1.954	1.868	1.743	1.586	1.402	WAFORD16
1.195	.967	.729	.490	.250	.009					WAFORD16
0.0	.304	.368	.469	.647	.875	1.059	1.213	1.459	1.645	WAFORD19
1.788	1.892	1.962	1.997	1.996	1.954	1.868	1.743	1.586	1.402	WAFORD19
1.195	.967	.729	.490	.250	.009					WAFORD19
0.0	.304	.368	.469	.647	.875	1.059	1.213	1.459	1.645	WAFORD22
1.788	1.892	1.962	1.997	1.996	1.954	1.868	1.743	1.586	1.402	WAFORD22
1.195	.967	.729	.490	.250	.009					WAFORD22
0.0	.304	.368	.469	.647	.875	1.059	1.213	1.459	1.645	WAFORD25
1.788	1.892	1.962	1.997	1.996	1.954	1.868	1.743	1.586	1.402	WAFORD25
1.195	.967	.729	.490	.250	.009					WAFORD25
0.0	.304	.368	.469	.647	.875	1.059	1.213	1.459	1.645	WAFORD28
1.788	1.892	1.962	1.997	1.996	1.954	1.868	1.743	1.586	1.402	WAFORD28
1.195	.967	.729	.490	.250	.009					WAFORD28
0.0	.304	.368	.469	.647	.875	1.059	1.213	1.459	1.645	WAFORD28
1.788	1.892	1.962	1.997	1.996	1.954	1.868	1.743	1.586	1.402	WAFORD28
1.195	.967	.729	.490	.250	.009					WAFORD28
0.0	.304	.368	.469	.647	.875	1.059	1.213	1.459	1.645	WAFORD29
1.788	1.892	1.962	1.997	1.996	1.954	1.868	1.743	1.586	1.402	WAFORD29
1.195	.967	.729	.490	.250	.009					WAFORD29
0.0	.304	.368	.469	.647	.875	1.059	1.213	1.459	1.645	WAFORD30
1.788	1.892	1.962	1.997	1.996	1.954	1.868	1.743	1.586	1.402	WAFORD30
1.195	.967	.729	.490	.250	.009					WAFORD30
0.0	.304	.368	.469	.647	.875	1.059	1.213	1.459	1.645	WAFORD31
1.788	1.892	1.962	1.997	1.996	1.954	1.868	1.743	1.586	1.402	WAFORD31
1.195	.967	.729	.490	.250	.009					WAFORD31
15.240	17.780	20.320	25.400	30.480	35.560	40.640	45.720			XFUS 9
-.139	-.239	-.339	-.539	-.738	-.938	-1.137	-1.337			ZFUS 9
15.518	15.518	15.518	15.518	15.518	15.518	15.518	15.518			FUSARD 9
46.736	50.800	55.880	60.960	66.040	68.580					XFUS 6
-1.377	-1.537	-1.736	-1.936	-2.135	-2.235					ZFUS 6
15.518	15.518	15.518	15.518	15.518	15.518					FUSARD 6

TABLE I.- Continued

(b) Geometry of cambered and twisted canard

0.0	.125	.25	.5	.75	1.0	1.5	2.5	5.0	10.0	XAF	10
15.0	20.0	30.0	40.0	50.0	60.0	70.0	80.0	90.0	100.0	XAF	20
8.994	5.164	.072	14.392							AFORG	1
10.782	6.198	-.199	13.111							AFORG	2
12.573	7.231	-.390	11.834							AFORG	3
14.361	8.263	-.491	10.554							AFORG	4
16.152	9.296	-.508	9.274							AFORG	5
17.940	10.330	-.508	7.993							AFORG	6
19.728	11.361	-.508	6.713							AFORG	7
21.519	12.395	-.508	5.436							AFORG	8
23.307	13.429	-.508	4.155							AFORG	9
24.686	14.224	-.508	3.170							AFORG	10
0.0	-.0009	-.0019	-.0044	-.0069	-.0088	-.0139	-.0207	-.0395	-.0664	CAMORD	1
-.0803	-.0810	-.0304	.2380	.2380	.2380	.2380	.2380	.2380	.2380	CAMORD	1
0.0	-.0001	-.0002	-.0003	-.0011	-.0013	-.0016	-.0029	-.0034	-.0014	CAMORD	2
.0100	.0290	.0943	.1458	.3416	.5704	1.4280	1.4280	1.4280	1.4280	CAMORD	2
0.0	-.0003	.0001	.0002	.0004	-.0002	.0001	.0005	.0017	.0060	CAMORD	3
.0128	.0235	.0523	.0777	.1653	.2600	.3895	.5574	.7787	.7787	CAMORD	3
0.0	0.0	0.0	0.0	0.0	.0020	.0030	.0050	.0080	.0180	CAMORD	4
.0279	.0406	.0686	.1016	.1397	.1480	.2439	.3150	.4039	.5131	CAMORD	4
0.0	0.0	0.0	0.0	0.0	0.0	.0020	.0030	.0050	.0100	CAMORD	5
.0203	.0279	.0457	.0660	.0849	.1148	.1473	.1803	.2184	.2616	CAMORD	5
0.0	0.0	0.0	0.0	0.0	0.0	0.0	.0030	.0050	.0080	CAMORD	6
.0130	.0178	.0305	.0457	.0559	.0752	.0940	.1143	.1346	.1600	CAMORD	6
0.0	0.0	0.0	0.0	0.0	0.0	0.0	.0020	.0030	.0050	CAMORD	7
.0102	.0130	.0200	.0310	.0381	.0483	.0610	.0737	.0864	.1016	CAMORD	7
0.0	0.0	0.0	0.0	0.0	0.0	0.0	0.0	.0025	.0050	CAMORD	8
.0076	.0102	.0152	.0203	.0254	.0330	.0406	.0483	.0564	.0635	CAMORD	8
0.0	0.0	0.0	0.0	0.0	0.0	0.0	0.0	.0012	.0038	CAMORD	9
.0044	.0056	.0102	.0130	.0178	.0203	.0254	.0305	.0330	.0381	CAMORD	9
0.0	0.0	0.0	0.0	0.0	0.0	0.0	0.0	0.0	0.0	CAMORD10	
.0006	.0019	.0031	.0038	.0044	.0050	.0057	.0071	.0086	.0102	CAMORD10	

TABLE I.- Concluded

(b) Concluded

0.0	.139	.210	.311	.378	.432	.525	.656	.877	1.216	AFORD	1
1.463	1.649	1.894	1.996	1.952	1.742	1.400	.966	.490	.009	AFORD	1
0.0	.139	.210	.311	.378	.432	.525	.656	.877	1.216	AFORD	2
1.463	1.649	1.894	1.996	1.952	1.742	1.400	.966	.490	.009	AFORD	2
0.0	.139	.210	.311	.378	.432	.525	.656	.877	1.216	AFORD	3
1.463	1.649	1.894	1.996	1.952	1.742	1.400	.966	.490	.009	AFORD	3
0.0	.139	.210	.311	.378	.432	.525	.656	.877	1.216	AFORD	4
1.463	1.649	1.894	1.996	1.952	1.742	1.400	.966	.490	.009	AFORD	4
0.0	.139	.210	.311	.378	.432	.525	.656	.877	1.216	AFORD	5
1.463	1.649	1.894	1.996	1.952	1.742	1.400	.966	.490	.009	AFORD	5
0.0	.139	.210	.311	.378	.432	.525	.656	.877	1.216	AFORD	6
1.463	1.649	1.894	1.996	1.952	1.742	1.400	.966	.490	.009	AFORD	6
0.0	.139	.210	.311	.378	.432	.525	.656	.877	1.216	AFORD	7
1.463	1.649	1.894	1.996	1.952	1.742	1.400	.966	.490	.009	AFORD	7
0.0	.139	.210	.311	.378	.432	.525	.656	.877	1.216	AFORD	8
1.463	1.649	1.894	1.996	1.952	1.742	1.400	.966	.490	.009	AFORD	8
0.0	.139	.210	.311	.378	.432	.525	.656	.877	1.216	AFORD	9
1.463	1.649	1.894	1.996	1.952	1.742	1.400	.966	.490	.009	AFORD	9
0.0	.139	.210	.311	.378	.432	.525	.656	.877	1.216	AFORD	10
1.463	1.649	1.894	1.996	1.952	1.742	1.400	.966	.490	.009	AFORD	10

TABLE II.- MEASURED STATIC LONGITUDINAL AERODYNAMIC CHARACTERISTICS

(a) Model without canards

M	α , deg	C_L	C_D	C_m	L/D	$C_{D,c}$
1.50	-3.99	-.1153	.0185	.0355	-6.2395	.0015
	-3.00	-.0680	.0153	.0281	-4.4372	.0015
	-1.99	-.0193	.0137	.0212	-1.4144	.0015
	-.96	.0300	.0135	.0133	2.2261	.0016
	.01	.0718	.0143	.0072	5.0055	.0016
	1.00	.1183	.0163	.0004	7.2614	.0016
	2.00	.1667	.0195	-.0069	8.5425	.0016
	4.01	.2654	.0311	-.0232	8.5405	.0015
	6.03	.3569	.0494	-.0322	7.2212	.0015
	8.00	.4416	.0754	-.0326	5.8539	.0015
	10.01	.5225	.1070	-.0351	4.8827	.0015
	12.03	.6051	.1456	-.0369	4.1556	.0016
	-.01	.0731	.0141	.0072	5.1956	.0016
	15.02	.7221	.2127	-.0373	3.3942	.0016
	15.00	.7203	.2118	-.0374	3.4005	.0016
1.80	-4.01	-.0959	.0173	.0302	-5.5424	.0015
	-3.00	-.0542	.0145	.0245	-3.7447	.0016
	-2.01	-.0116	.0130	.0188	-.8904	.0016
	-1.01	.0299	.0129	.0134	2.3211	.0016
	.00	.0713	.0139	.0083	5.1461	.0016
	.98	.1111	.0158	.0036	7.0455	.0017
	2.01	.1544	.0190	-.0022	8.1217	.0016
	4.00	.2354	.0297	-.0119	7.9283	.0016
	6.00	.3138	.0462	-.0165	6.7989	.0015
	8.01	.3837	.0685	-.0165	5.5991	.0015
	10.01	.4540	.0962	-.0174	4.7177	.0015
	11.99	.5212	.1283	-.0190	4.0622	.0015
	16.00	.6518	.2076	-.0209	3.1392	.0014
	.01	.0722	.0138	.0083	5.2223	.0016
2.00	-4.01	-.0880	.0167	.0261	-5.2632	.0014
	-2.99	-.0486	.0140	.0211	-3.4606	.0014
	-1.99	-.0094	.0128	.0164	-.7335	.0015
	-.95	.0318	.0127	.0114	2.5000	.0015
	.02	.0679	.0137	.0074	4.9586	.0015
	1.03	.1068	.0158	.0033	6.7696	.0015
	2.01	.1433	.0189	-.0011	7.5943	.0015
	4.00	.2205	.0293	-.0082	7.5354	.0015
	6.02	.2896	.0447	-.0102	6.4737	.0014
	8.01	.3556	.0655	-.0111	5.4253	.0014
	10.01	.4201	.0910	-.0120	4.6177	.0014
	11.99	.4817	.1207	-.0126	3.9917	.0014
	16.02	.6005	.1939	-.0134	3.0973	.0013
	19.99	.7110	.2832	-.0145	2.5105	.0013
	.01	.0716	.0138	.0075	5.1968	.0015

TABLE II.- Continued

(b) Model with cambered and twisted canard

M	δ_f , deg	α , deg	C_L	C_D	C_m	L/D	$C_{D,c}$
1.50	0	-8.79	-.2589	.0609	.0134	-5.8938	.0017
		-6.81	-.2651	.0396	.0156	-6.4854	.0016
		-5.83	-.2191	.0314	.0151	-6.9480	.0016
		-4.81	-.1690	.0244	.0138	-6.9196	.0016
		-3.80	-.1165	.0192	.0133	-6.0754	.0016
		-2.77	-.0647	.0153	.0122	-4.0805	.0016
		-.80	.0332	.0143	.0095	2.3195	.0016
		1.19	.1258	.0177	.0075	7.1049	.0016
		3.20	.2284	.0272	.0049	8.4002	.0016
		5.18	.3250	.0434	.0029	7.4849	.0016
		7.22	.4205	.0676	.0074	6.2230	.0016
		11.20	.5938	.1335	.0223	4.4464	.0016
		14.25	.7217	.2011	.0322	3.5892	.0017
		-4.30	-.1652	.0241	.0145	-6.8457	.0016
		-1.78	-.0134	.0143	.0113	-.9398	.0016
		.23	.0842	.0156	.0090	5.4502	.0016
1.50	0.5	-4.03	-.1279	.0200	.0143	-6.4008	.0016
		-1.94	-.0225	.0142	.0121	-1.5791	.0016
		-.99	.0235	.0140	.0108	1.6824	.0016
		.02	.0717	.0149	.0097	4.7985	.0016
		1.00	.1193	.0170	.0084	7.0341	.0016
		2.01	.1700	.0204	.0078	8.3163	.0016
		4.02	.2719	.0331	.0044	8.2239	.0016
		6.00	.3644	.0521	.0058	6.9948	.0016
		8.00	.4548	.0785	.0109	5.7951	.0016
		10.00	.5397	.1107	.0187	4.8770	.0016
		12.01	.6266	.1495	.0258	4.1907	.0016
		14.00	.7088	.1940	.0315	3.6525	.0017
		.01	.0719	.0148	.0097	4.8480	.0016
		-2.93	-.0748	.0161	.0131	-4.6525	.0016
1.50	-0.5	-4.03	-.1273	.0204	.0123	-6.2524	.0016
		-3.04	-.0780	.0168	.0110	-4.6570	.0016
		-2.00	-.0260	.0148	.0102	-1.7612	.0016
		-.99	.0249	.0144	.0095	1.7301	.0016
		.01	.0732	.0154	.0084	4.7627	.0016
		.99	.1200	.0173	.0068	6.9241	.0016
		1.94	.1682	.0207	.0056	8.1133	.0016
		4.00	.2724	.0334	.0030	8.1658	.0016
		6.00	.3667	.0525	.0042	6.9838	.0016
		7.93	.4548	.0786	.0094	5.7900	.0016
		9.99	.5404	.1108	.0172	4.8782	.0016
		12.01	.6266	.1498	.0242	4.1641	.0016
		15.00	.7526	.2202	.0359	3.4176	.0017
		.01	.0739	.0153	.0085	4.8334	.0016

TABLE II.- Continued

(b) Continued

M	δ_f , deg	α , deg	C_L	C_D	C_m	L/D	$C_{D,c}$
1.50	-1.5	-3.98	-.1230	.0200	.0117	-6.1406	.0016
		-2.98	-.0740	.0166	.0104	-4.4629	.0016
		-1.99	-.0255	.0147	.0091	-1.7402	.0015
		-0.97	.0258	.0144	.0082	1.7973	.0016
		.03	.0740	.0153	.0070	4.8425	.0016
		1.01	.1203	.0173	.0060	6.9632	.0016
		2.01	.1703	.0208	.0048	8.2043	.0016
		4.01	.2714	.0331	.0019	8.1991	.0016
		6.02	.3687	.0527	.0036	6.9954	.0016
		7.98	.4566	.0785	.0081	5.8158	.0016
		9.99	.5434	.1110	.0171	4.8949	.0016
		12.01	.6287	.1499	.0237	4.1930	.0016
		15.02	.7512	.2196	.0340	3.4206	.0017
		.02	.0721	.0152	.0070	4.7345	.0016
1.50	-2.5	-4.00	-.1260	.0204	.0109	-6.1711	.0015
		-3.04	-.0794	.0169	.0091	-4.6876	.0015
		-2.01	-.0271	.0149	.0083	-1.8207	.0015
		-1.02	.0222	.0144	.0070	1.5436	.0016
		.01	.0703	.0152	.0060	4.6262	.0016
		1.02	.1184	.0172	.0043	6.8870	.0016
		1.99	.1676	.0205	.0034	8.1908	.0016
		4.00	.2705	.0327	-.0005	8.2635	.0016
		6.03	.3688	.0524	.0019	7.0315	.0016
		8.00	.4566	.0783	.0067	5.8322	.0016
		10.01	.5425	.1106	.0150	4.9055	.0016
		12.03	.6280	.1496	.0228	4.1977	.0016
		15.00	.7502	.2187	.0340	3.4296	.0017
		.02	.0706	.0150	.0058	4.6998	.0016

TABLE II.- Continued

(b) Continued

M	δ_f , deg	α , deg	C_L	C_D	C_m	L/D	$C_{D,c}$
1.80	0	-4.74	-.1461	.0226	.0131	-6.4682	.0016
		-8.47	-.3011	.0512	.0104	-5.8755	.0016
		-6.47	-.2209	.0336	.0130	-6.5662	.0015
		-4.45	-.1330	.0211	.0132	-6.3021	.0016
		-2.43	-.0437	.0147	.0113	-2.9729	.0016
		-1.45	.0019	.0138	.0105	.1374	.0016
		-.48	.0461	.0141	.0100	3.2591	.0017
		.52	.0909	.0158	.0096	5.7687	.0017
		1.49	.1314	.0184	.0088	7.1505	.0017
		3.52	.2204	.0285	.0082	7.7346	.0017
		5.51	.3051	.0445	.0100	6.8540	.0017
		7.55	.3858	.0665	.0143	5.8020	.0016
		11.54	.5347	.1266	.0280	4.2244	.0016
		15.52	.6733	.2073	.0415	3.2483	.0016
		-4.47	-.1318	.0211	.0133	-6.2518	.0016
1.80	0.5	-4.00	-.1115	.0190	.0129	-5.8691	.0016
		-3.01	-.0652	.0157	.0121	-4.1577	.0016
		-2.01	-.0208	.0140	.0113	-1.4892	.0016
		-1.01	.0232	.0137	.0104	1.6920	.0016
		.01	.0671	.0147	.0094	4.5532	.0017
		1.01	.1107	.0170	.0092	6.5316	.0017
		2.00	.1545	.0204	.0088	7.5865	.0017
		3.99	.2410	.0317	.0081	7.5970	.0017
		6.00	.3258	.0494	.0106	6.5970	.0016
		8.01	.4034	.0721	.0152	5.5915	.0016
		10.01	.4773	.1006	.0224	4.7426	.0016
		12.03	.5514	.1353	.0297	4.0753	.0016
		16.03	.6897	.2191	.0436	3.1480	.0016
		.03	.0706	.0148	.0099	4.7568	.0017
1.80	-0.5	-4.00	-.1069	.0190	.0123	-5.6376	.0016
		-2.98	-.0626	.0157	.0111	-3.9778	.0016
		-2.00	-.0176	.0141	.0100	-1.2509	.0016
		-.99	.0269	.0138	.0096	1.9433	.0016
		-.02	.0692	.0148	.0089	4.6748	.0016
		.98	.1124	.0169	.0087	6.6356	.0016
		2.00	.1583	.0205	.0078	7.7357	.0016
		4.01	.2470	.0323	.0079	7.6548	.0016
		6.00	.3281	.0495	.0102	6.6315	.0016
		8.00	.4059	.0723	.0145	5.6119	.0016
		10.02	.4820	.1015	.0225	4.7493	.0016
		12.02	.5539	.1356	.0288	4.0834	.0016
		13.99	.6231	.1742	.0356	3.5762	.0016
		16.00	.6913	.2189	.0432	3.1580	.0015
		.01	.0730	.0149	.0090	4.8947	.0016

TABLE II.- Continued

(b) Continued

M	δ_f , deg	α , deg	C_L	C_D	C_m	L/D	$C_{D,c}$
1.80	-1.5	-3.99	-.1099	.0193	.0114	-5.6995	.0015
		-2.97	-.0617	.0159	.0104	-3.8849	.0016
		-1.98	-.0180	.0142	.0096	-1.2628	.0016
		-.97	.0285	.0140	.0090	2.0346	.0016
		.01	.0709	.0150	.0082	4.7275	.0016
		1.00	.1130	.0171	.0075	6.6230	.0016
		2.00	.1591	.0206	.0070	7.7372	.0016
		4.03	.2473	.0323	.0068	7.6465	.0016
		6.01	.3288	.0496	.0093	6.6321	.0016
		8.01	.4081	.0726	.0139	5.6194	.0016
		10.03	.4824	.1015	.0219	4.7525	.0015
		12.01	.5554	.1356	.0282	4.0952	.0016
		15.99	.6899	.2181	.0417	3.1635	.0015
		.01	.0728	.0149	.0082	4.8901	.0016
1.80	-2.5	-3.99	-.1113	.0195	.0106	-5.7213	.0015
		-2.99	-.0655	.0161	.0094	-4.0648	.0016
		-2.00	-.0224	.0144	.0084	-1.5566	.0016
		-.99	.0220	.0140	.0075	1.5767	.0016
		.02	.0665	.0149	.0072	4.4731	.0016
		1.00	.1094	.0168	.0061	6.4932	.0017
		2.00	.1537	.0202	.0055	7.5985	.0017
		4.01	.2429	.0318	.0054	7.6497	.0016
		6.00	.3249	.0489	.0079	6.6402	.0016
		8.02	.4038	.0719	.0129	5.6151	.0016
		10.02	.4775	.1002	.0199	4.7631	.0016
		12.01	.5510	.1343	.0271	4.1025	.0016
		16.04	.6888	.2182	.0411	3.1567	.0015
		.02	.0695	.0149	.0073	4.6742	.0016

TABLE II.- Continued

(b) Continued

M	δ_f , deg	α , deg	C_L	C_D	C_m	L/D	$C_{D,C}$
2.00	0	-8.91	-.2931	.0519	.0084	-5.6443	.0015
		-6.92	-.2198	.0343	.0114	-6.3131	.0014
		-4.90	-.1390	.0221	.0122	-6.3017	.0014
		-2.87	-.0545	.0149	.0105	-3.6679	.0015
		-1.90	-.0141	.0135	.0097	-1.0433	.0015
		-.91	.0290	.0134	.0094	2.1612	.0015
		.10	.0682	.0146	.0090	4.6686	.0016
		1.11	.1097	.0170	.0088	6.4667	.0016
		3.09	.1921	.0254	.0091	7.5524	.0016
		5.12	.2714	.0397	.0111	6.8318	.0015
		7.17	.3460	.0590	.0154	5.8662	.0015
		11.12	.4844	.1132	.0275	4.2807	.0015
		15.10	.6138	.1866	.0402	3.2883	.0014
		-4.90	-.1376	.0220	.0122	-6.2522	.0014
2.00	0.5	-3.99	-.0956	.0180	.0117	-5.3190	.0015
		-2.99	-.0541	.0150	.0106	-3.5951	.0015
		-2.02	-.0140	.0135	.0098	-1.0341	.0015
		-1.01	.0284	.0134	.0096	2.1184	.0015
		.00	.0695	.0145	.0093	4.7860	.0016
		1.00	.1089	.0168	.0088	6.4871	.0016
		2.00	.1490	.0203	.0090	7.3550	.0015
		4.01	.2299	.0314	.0099	7.3242	.0015
		6.01	.3054	.0478	.0130	6.3849	.0015
		8.00	.3791	.0695	.0182	5.4530	.0015
		10.00	.4454	.0957	.0240	4.6524	.0014
		12.00	.5128	.1276	.0309	4.0172	.0014
		16.04	.6418	.2065	.0433	3.1082	.0014
		18.02	.7012	.2516	.0490	2.7867	.0014
		.01	.0711	.0146	.0092	4.8551	.0016
2.00	-0.5	-4.01	-.1017	.0184	.0098	-5.5220	.0014
		-2.99	-.0583	.0153	.0093	-3.8064	.0015
		-2.00	-.0171	.0138	.0083	-1.2418	.0015
		-1.01	.0232	.0136	.0075	1.7071	.0015
		.01	.0661	.0147	.0073	4.5116	.0015
		1.03	.1055	.0168	.0073	6.2623	.0015
		2.03	.1479	.0204	.0074	7.2655	.0015
		4.01	.2273	.0312	.0081	7.2815	.0015
		5.99	.3035	.0475	.0114	6.3900	.0015
		8.01	.3780	.0694	.0164	5.4471	.0015
		10.02	.4479	.0954	.0232	4.6472	.0014
		12.01	.5130	.1277	.0290	4.0184	.0014
		16.01	.6419	.2059	.0422	3.1172	.0014
		18.04	.7022	.2518	.0476	2.7885	.0014
		.02	.0700	.0147	.0078	4.7700	.0015

TABLE II.-- Continued

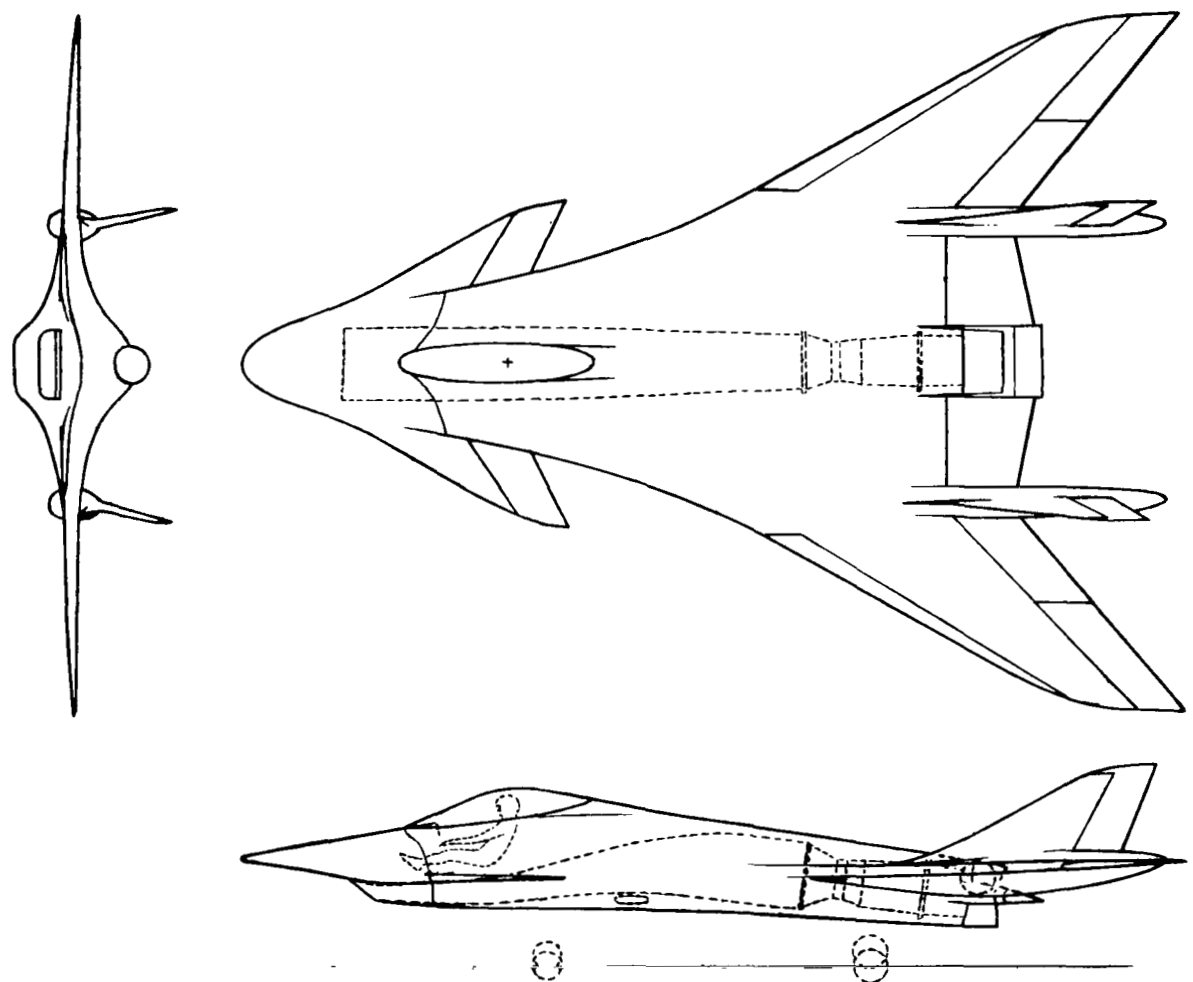
(b) Concluded

M	δ_f , deg	α , deg	C_L	C_D	C_m	L/D	C_D, c
2.00	-1.5	-3.99 -2.99 -2.00 -1.02 .03 1.02 2.00 3.99 6.00 8.01 10.03 12.02 16.00 18.00 .02	-.0982 -.0582 -.0160 .0243 .0677 .1080 .1474 .2286 .3053 .3793 .4495 .5147 .6420 .7025 .0691	.0185 .0155 .0139 .0137 .0148 .0170 .0203 .0312 .0477 .0694 .0966 .1279 .2056 .2511 .0147	.0078 .0070 .0064 .0060 .0060 .0058 .0060 .0069 .0107 .0157 .0227 .0287 .0410 .0467 .0060	-5.3216 -3.7509 -1.1502 1.7724 4.5838 6.3577 7.2761 7.3171 6.4037 5.4626 4.6533 4.0241 3.1221 2.7972 4.6843	.0014 .0015 .0015 .0015 .0015 .0015 .0015 .0015 .0015 .0015 .0014 .0014 .0014 .0014 .0015
2.00	-2.5	-4.02 -2.97 -1.97 -1.01 .01 .99 1.99 3.99 6.00 8.02 10.00 12.02 16.03 17.99 .01	-.0997 -.0567 -.0150 .0260 .0664 .1057 .1453 .2267 .3030 .3776 .4447 .5131 .6405 .6991 .0680	.0185 .0154 .0139 .0136 .0146 .0167 .0200 .0309 .0473 .0691 .0952 .1275 .2053 .2497 .0146	.0091 .0081 .0075 .0070 .0064 .0060 .0058 .0070 .0104 .0156 .0220 .0286 .0405 .0456 .0068	-5.3797 -3.6826 -1.0783 1.9057 4.5406 6.3305 7.2533 7.3299 6.4083 5.4652 4.6704 4.0245 3.1196 2.7998 4.6440	.0014 .0015 .0015 .0015 .0015 .0015 .0015 .0015 .0015 .0014 .0014 .0014 .0014 .0014 .0015

TABLE II.- Concluded

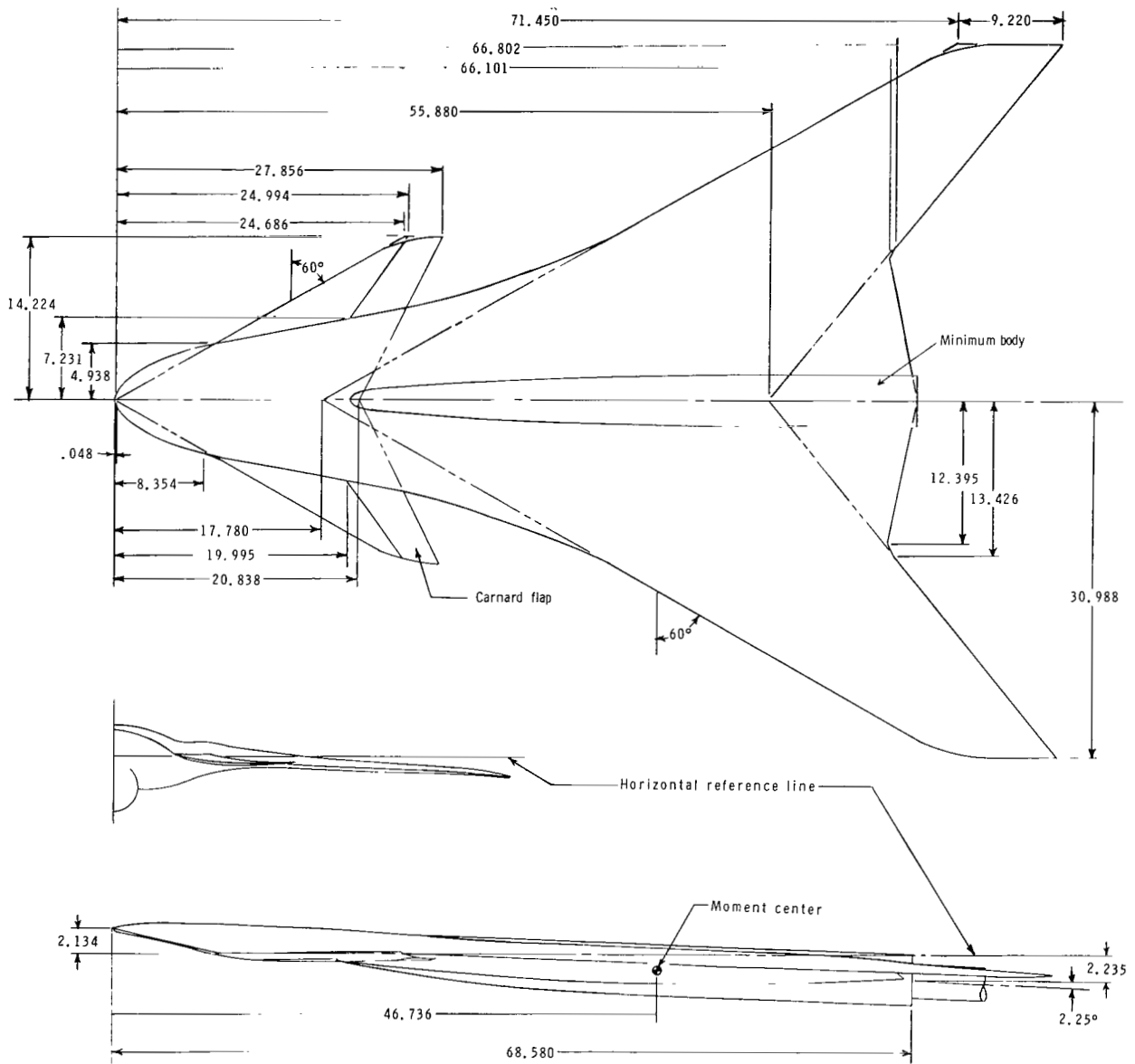
(c) Model with flat canard

M	α , deg	C_L	C_D	C_m	L/D	$C_{D,c}$
1.50	-4.02	-.1179	.0197	.0190	-5.9921	.0015
	-2.00	-.0204	.0148	.0164	-1.3737	.0015
	-1.00	.0253	.0147	.0150	1.7255	.0015
	.04	.0757	.0157	.0141	4.7863	.0015
	1.04	.1196	.0177	.0136	6.7383	.0015
	2.01	.1661	.0211	.0128	7.8546	.0015
	4.01	.2678	.0337	.0091	7.9542	.0015
	6.04	.3651	.0535	.0093	6.8300	.0015
	8.02	.4564	.0800	.0147	5.7060	.0015
	10.01	.5412	.1124	.0230	4.8160	.0015
	12.02	.6252	.1508	.0297	4.1466	.0016
	14.11	.7148	.1984	.0355	3.6033	.0016
	-.01	.0725	.0155	.0144	4.6741	.0015
1.80	-4.00	-.1069	.0188	.0170	-5.6886	.0015
	-2.01	-.0178	.0142	.0146	-1.2500	.0016
	-1.01	.0251	.0141	.0143	1.7746	.0016
	.03	.0684	.0152	.0137	4.4883	.0017
	1.01	.1066	.0172	.0133	6.1798	.0016
	2.00	.1524	.0207	.0133	7.3586	.0016
	4.02	.2412	.0325	.0127	7.4297	.0016
	6.02	.3252	.0500	.0148	6.5101	.0015
	8.03	.4029	.0729	.0191	5.5242	.0015
	10.02	.4805	.1021	.0258	4.7081	.0015
	12.03	.5528	.1362	.0324	4.0586	.0015
	16.04	.6930	.2207	.0457	3.1402	.0015
	18.04	.7595	.2704	.0516	2.8083	.0015
	.00	.0678	.0152	.0137	4.4618	.0017
2.00	-3.99	-.0941	.0178	.0155	-5.2772	.0014
	-2.01	-.0130	.0138	.0136	-.9413	.0015
	-1.04	.0255	.0137	.0133	1.8585	.0015
	-.01	.0664	.0149	.0137	4.4507	.0016
	1.03	.1049	.0171	.0135	6.1509	.0015
	1.99	.1443	.0203	.0131	7.0938	.0016
	4.02	.2272	.0316	.0132	7.1837	.0015
	6.00	.3033	.0479	.0159	6.3262	.0014
	8.01	.3781	.0700	.0209	5.4047	.0014
	10.02	.4471	.0967	.0266	4.6238	.0014
	12.02	.5141	.1286	.0330	3.9987	.0013
	16.04	.6456	.2080	.0450	3.1043	.0013
	19.05	.7379	.2794	.0530	2.6409	.0013
	.01	.0676	.0149	.0133	4.5226	.0016



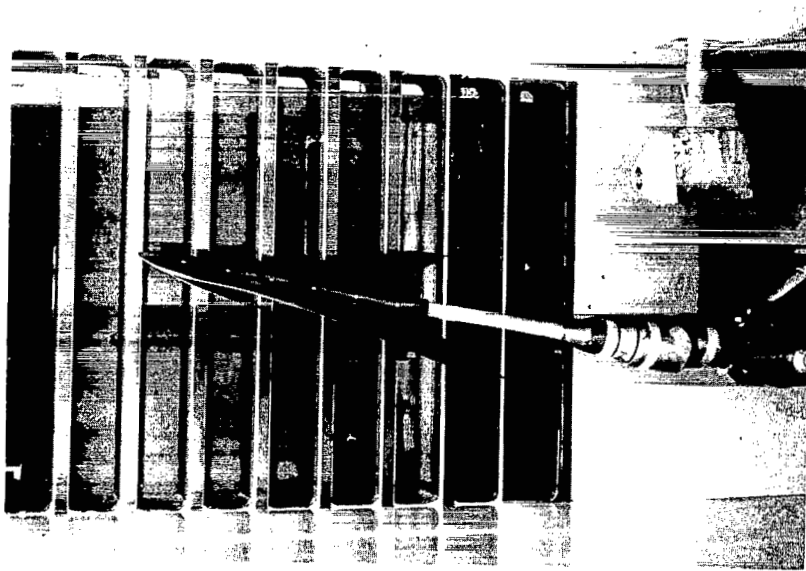
(a) Aircraft concept.

Figure 1.- Drawings of aircraft concept and wind-tunnel model.

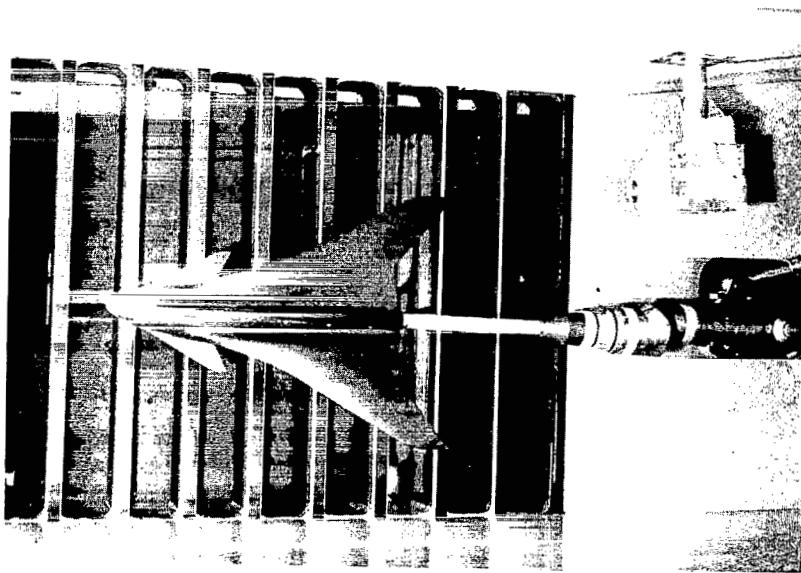


(b) Details of wind-tunnel model. Dimensions are in centimeters.

Figure 1.- Concluded.

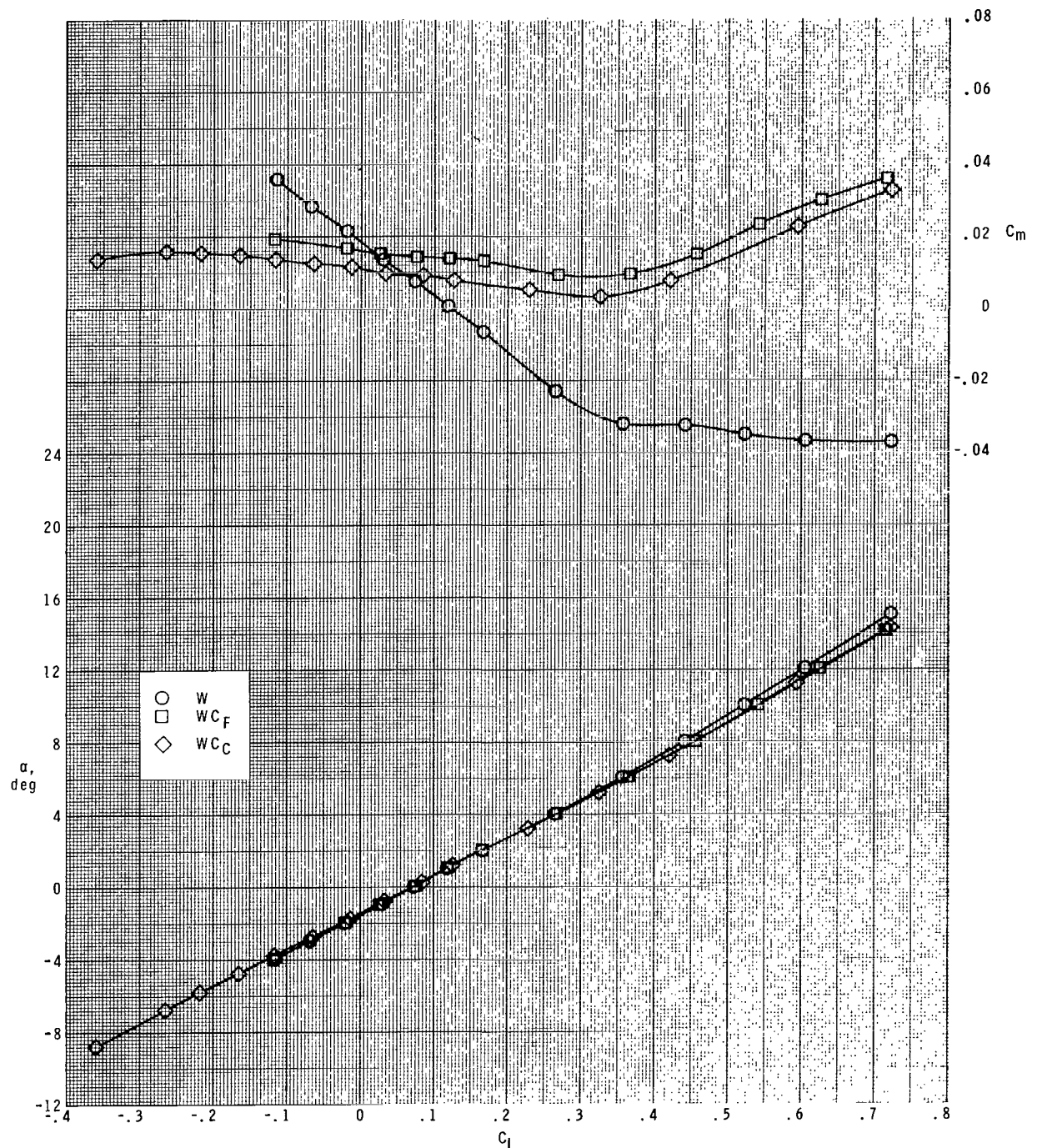


L-77-6067



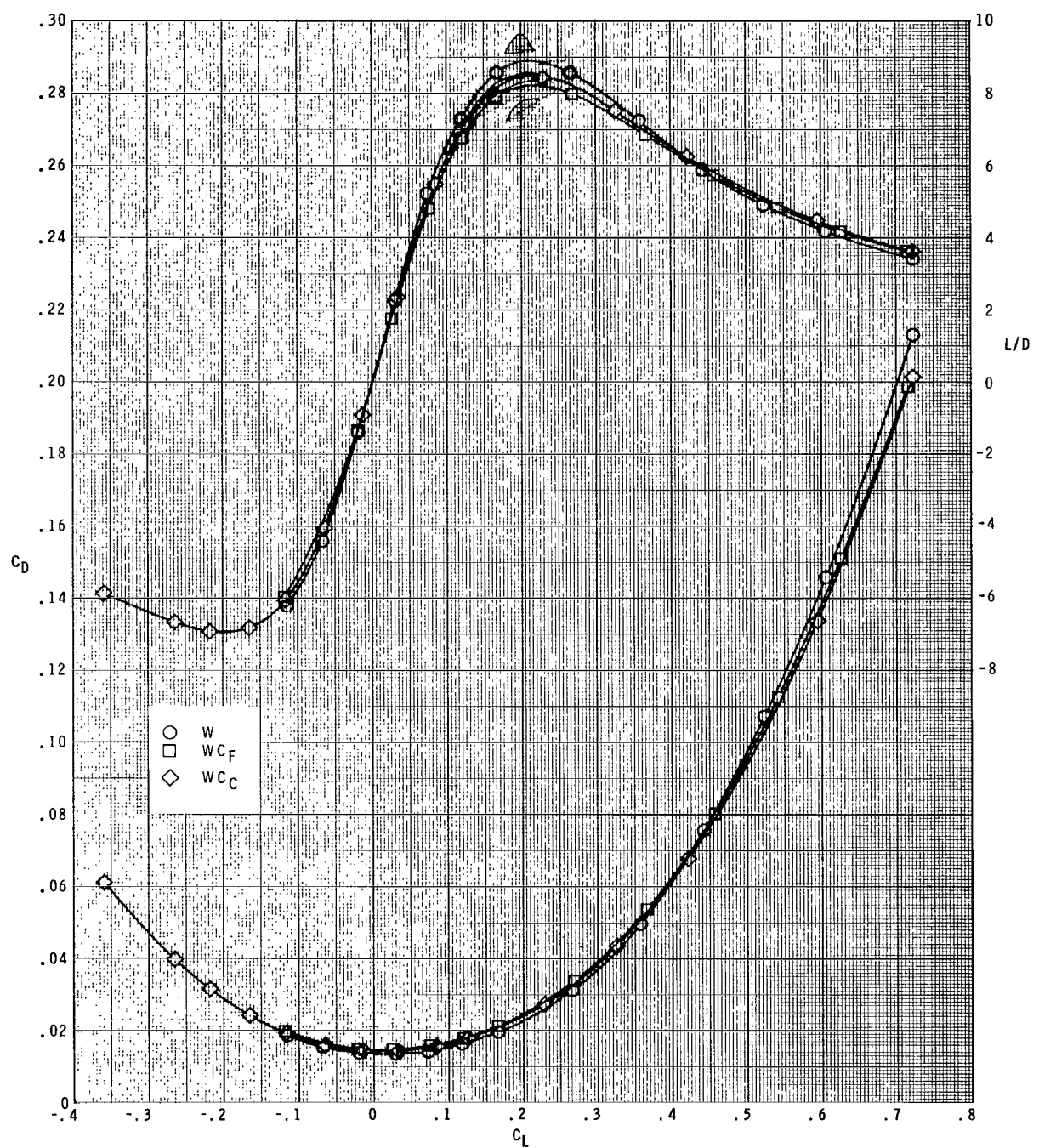
L-77-6066

Figure 2.- Model with canards installed in Langley Unitary Plan wind tunnel.



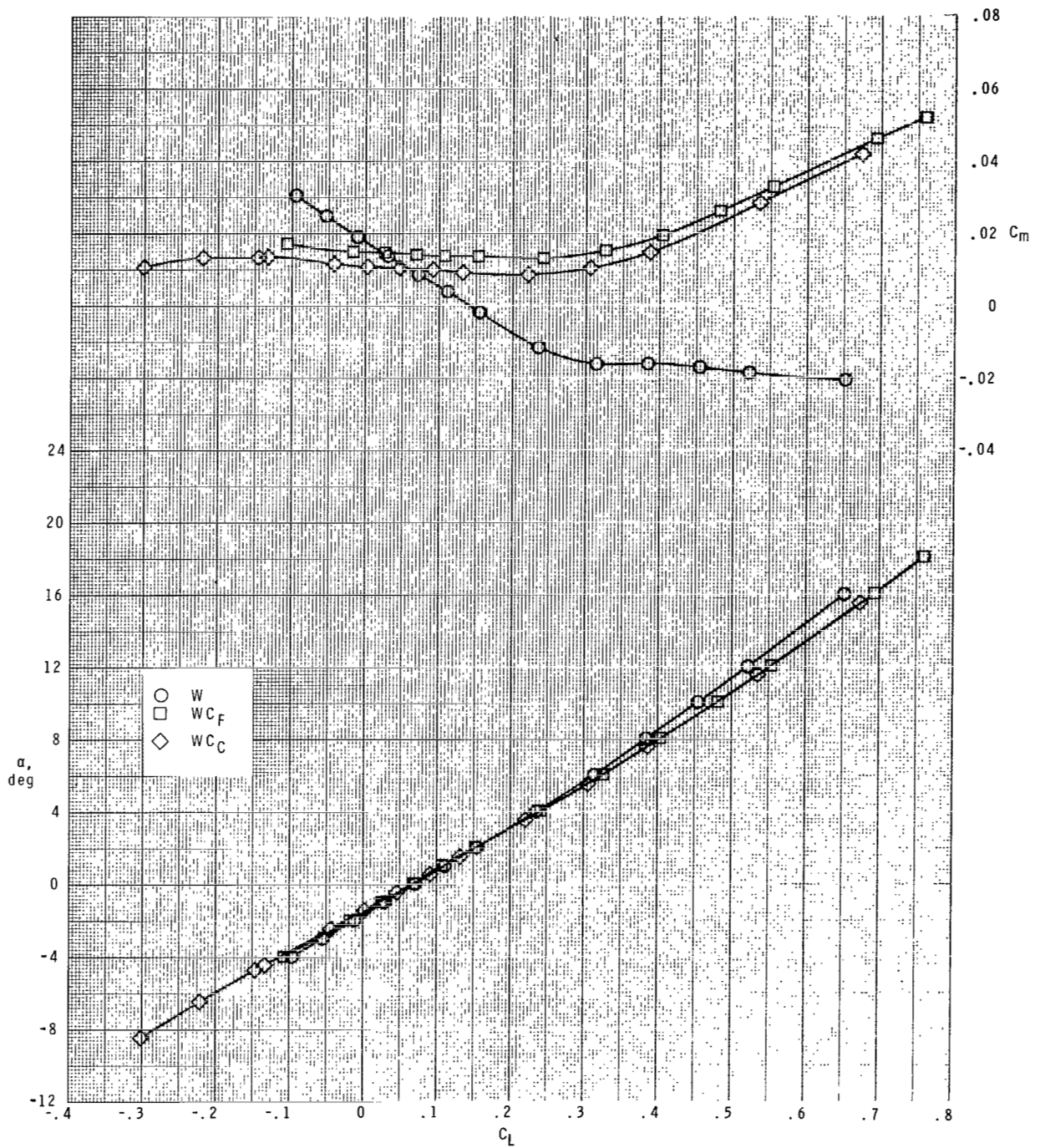
(a) $M = 1.5$.

Figure 3.- Longitudinal aerodynamic characteristics.



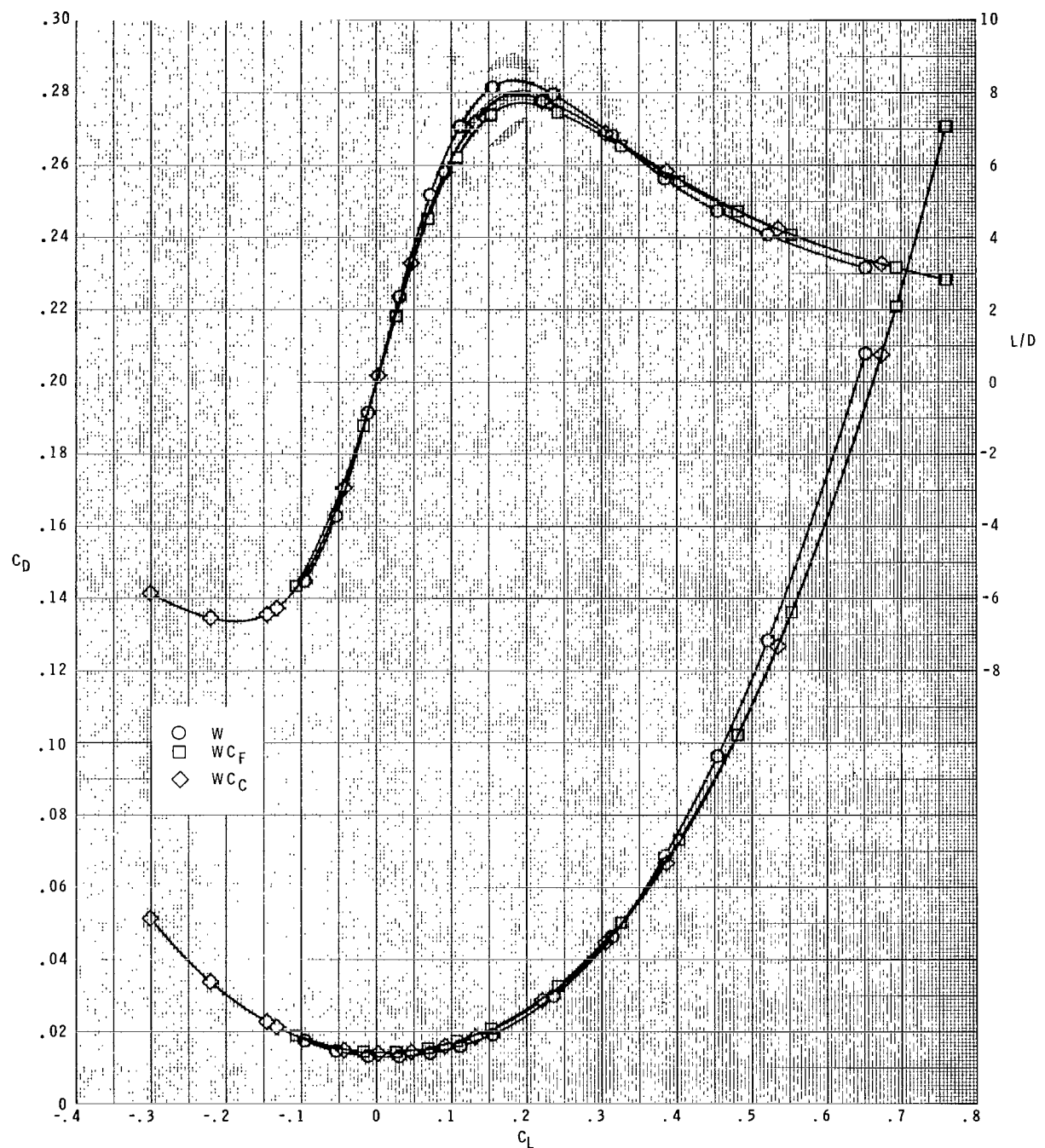
(a) Concluded.

Figure 3.- Continued.



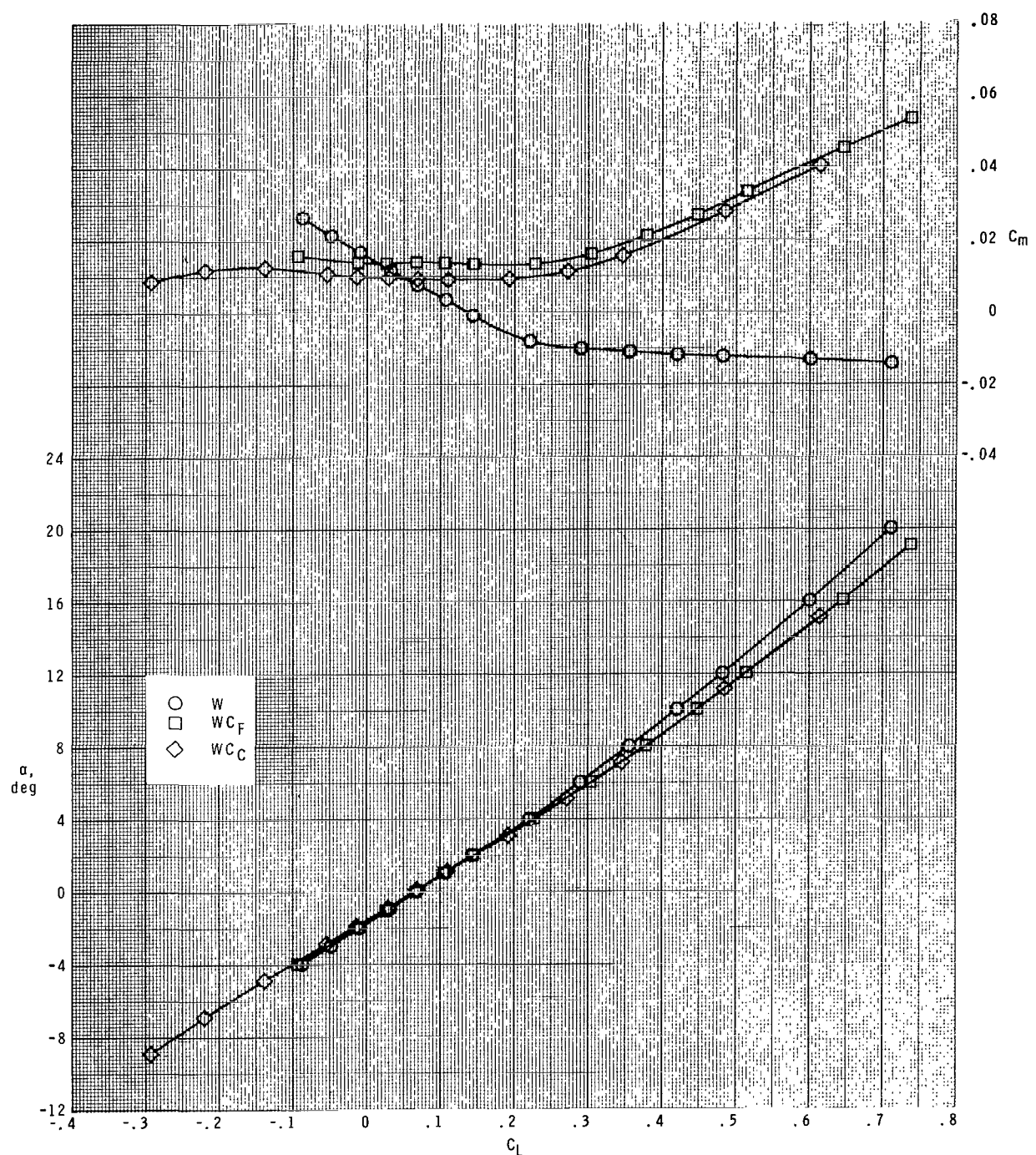
(b) $M = 1.8.$

Figure 3.- Continued.



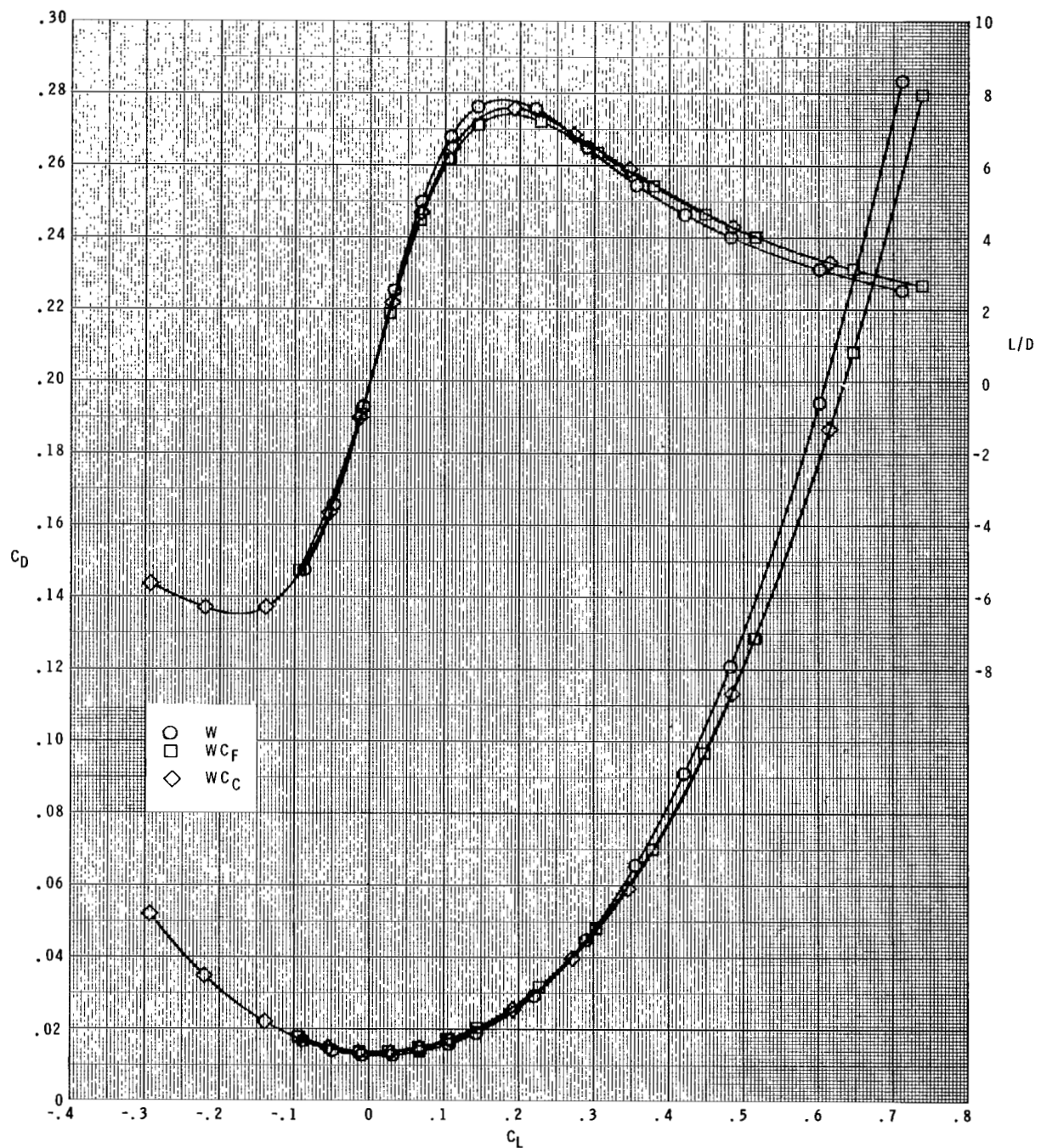
(b) Concluded.

Figure 3.- Continued.



(c) $M = 2.0$.

Figure 3.- Continued.



(c) Concluded.

Figure 3.- Concluded.

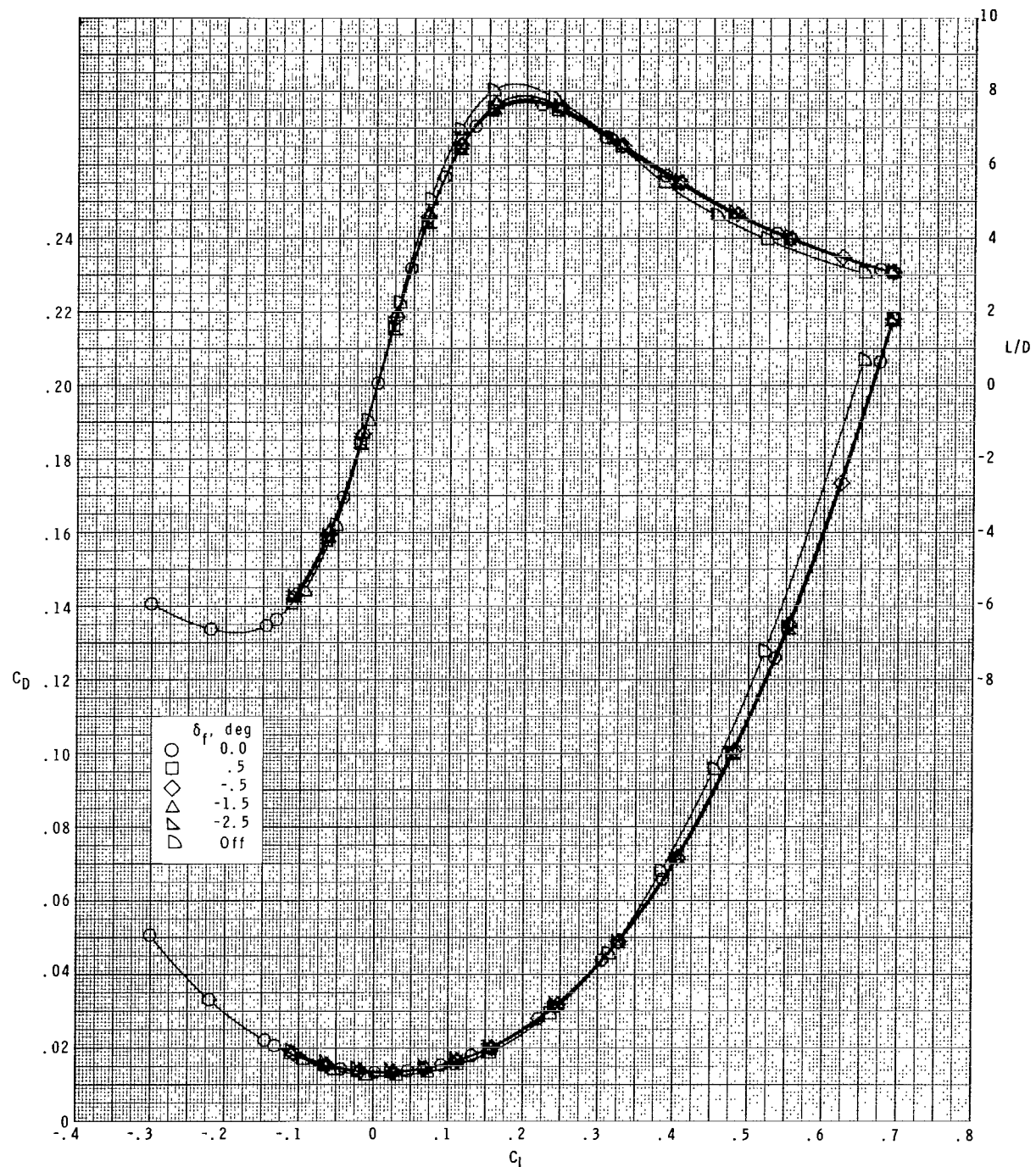


Figure 4.- Effect on longitudinal aerodynamic characteristics of small variations in flap deflection of cambered canard at $M = 1.8$.

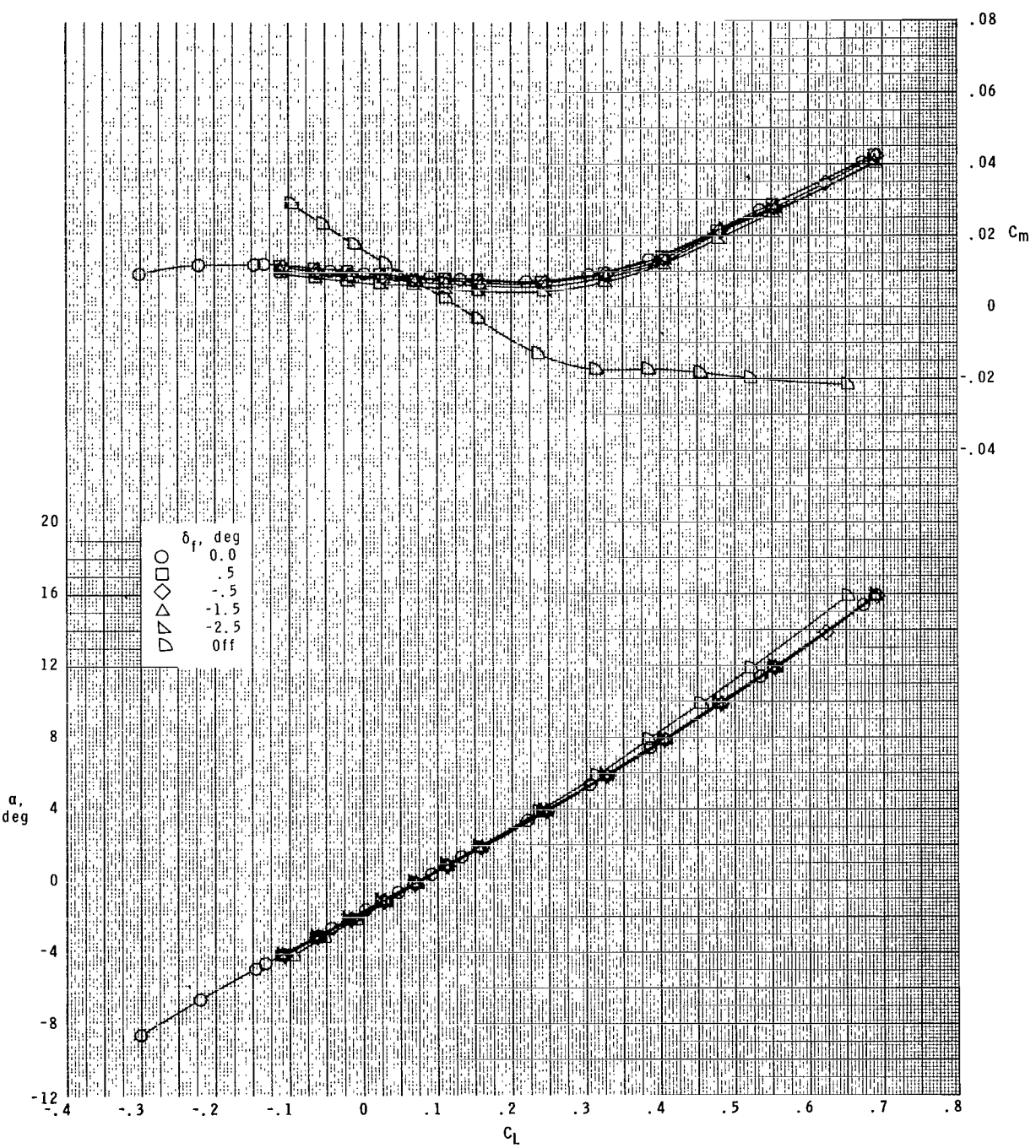
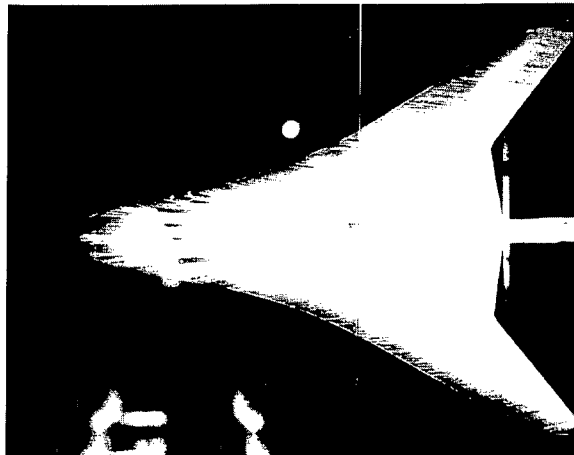
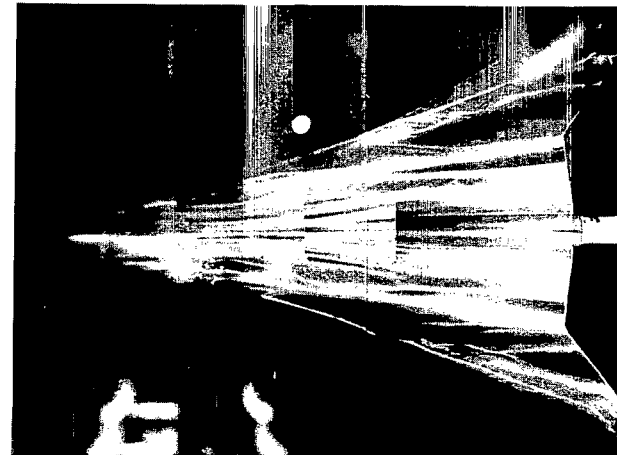
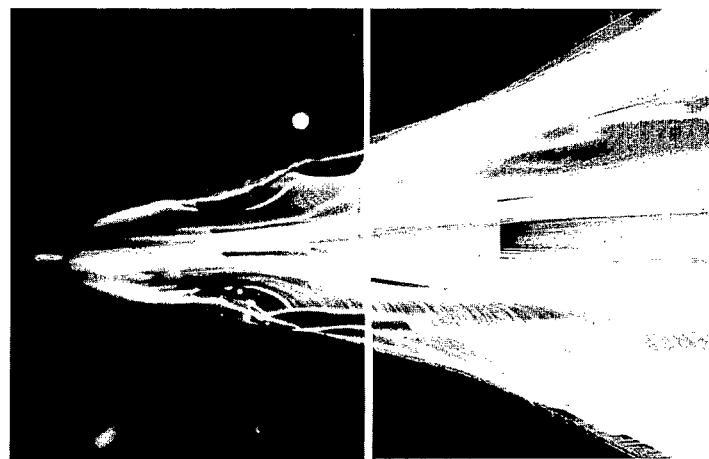
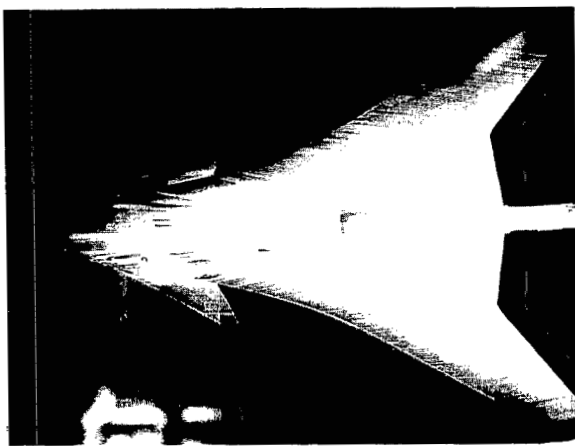
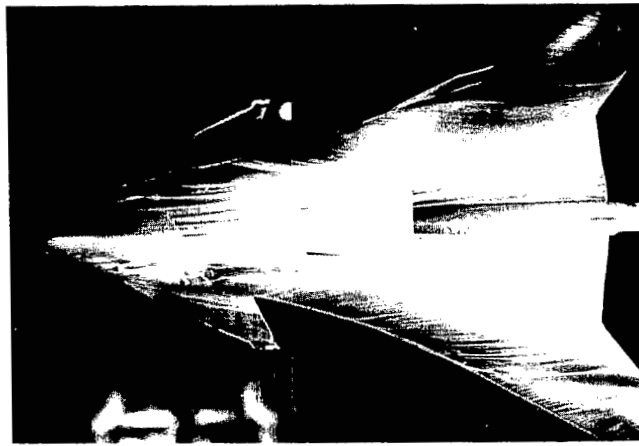
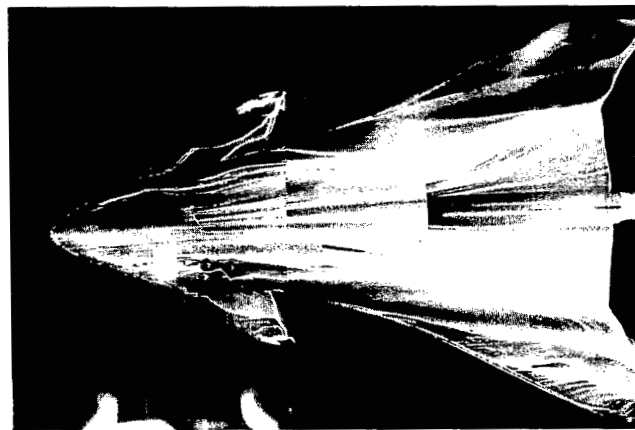


Figure 4.- Concluded.

 $\alpha = 0^\circ$  $\alpha = 4^\circ$  $\alpha = 8^\circ$

L-79-125

Figure 5.- Oil-flow photographs of configuration without canards at $M = 1.8$.

 $\alpha = 0^\circ$  $\alpha = 4^\circ$  $\alpha = 8^\circ$

L-79-126

Figure 6.- Oil-flow photographs of configuration with cambered canards at $M = 1.8$.



$\alpha = 12^\circ$

L-79-127

Figure 6.- Concluded.

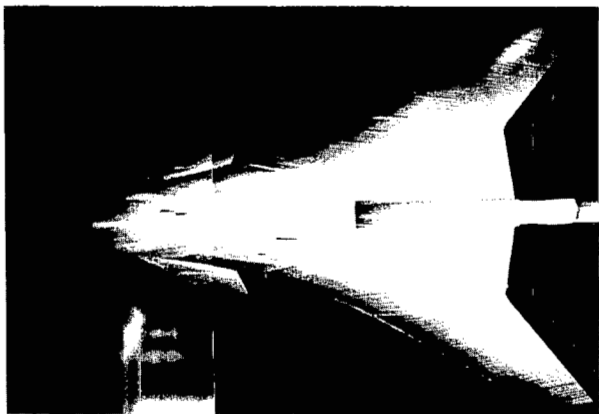
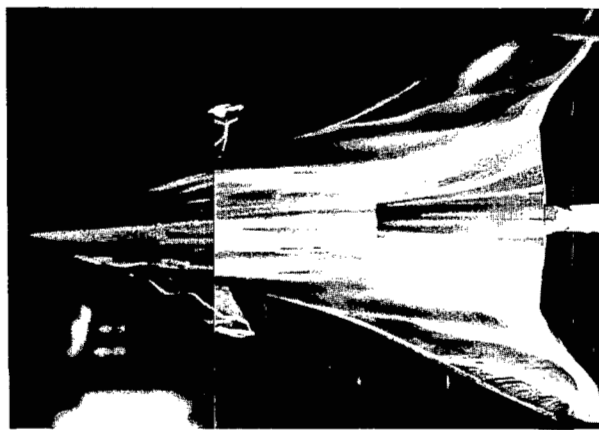
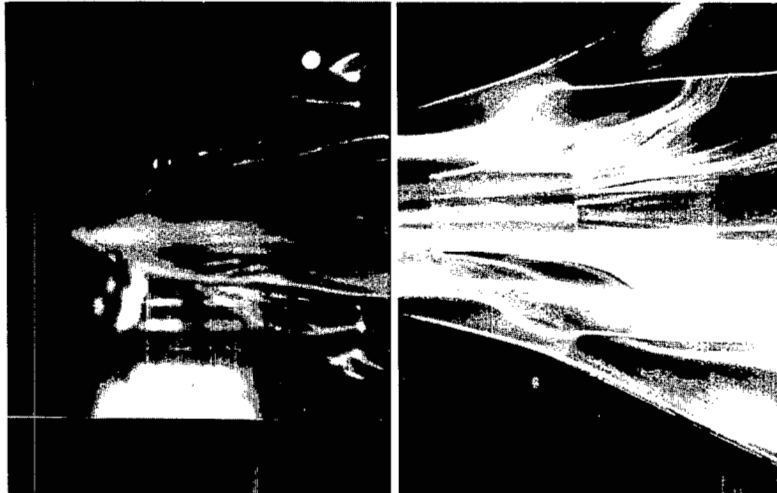
 $\alpha = 0^\circ$  $\alpha = 4^\circ$  $\alpha = 8^\circ$  $\alpha = 12^\circ$

Figure 7.- Oil-flow photographs of configuration with flat canards at $M = 1.8$.

L-79-128



$x = 10.16$



$x = 20.32$



$x = 30.48$



$x = 40.64$



$x = 50.80$

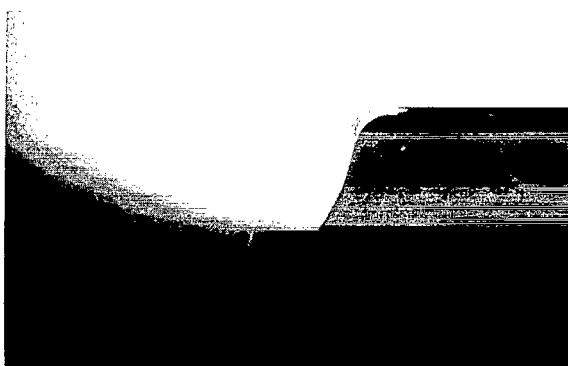


$x = 60.96$

(a) $\alpha = 4^\circ$.

L-79-129

Figure 8.- Vapor-screen photographs of configuration without canards
at $M = 1.8$.



$x = 10.16$



$x = 20.32$



$x = 30.48$



$x = 40.64$



$x = 50.80$

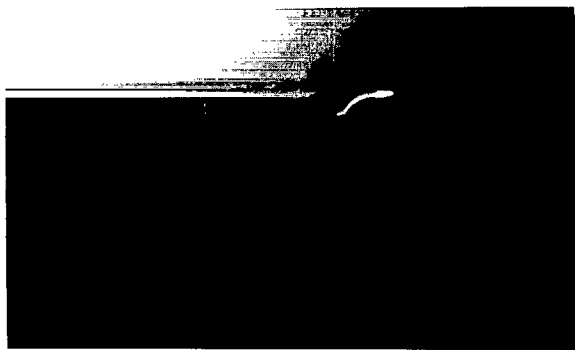


$x = 60.96$

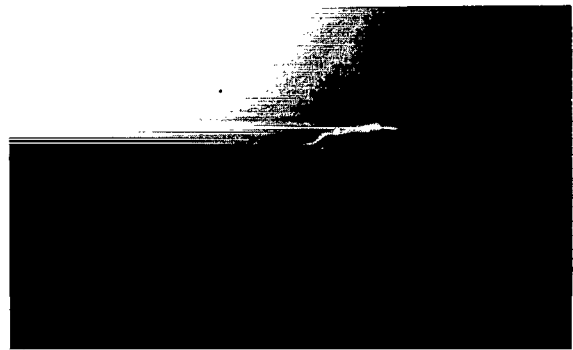
(b) $\alpha = 12^\circ$.

L-79-130

Figure 8.- Concluded.



$x = 10.16$



$x = 20.32$



$x = 30.48$



$x = 40.64$



$x = 50.80$



$x = 60.96$

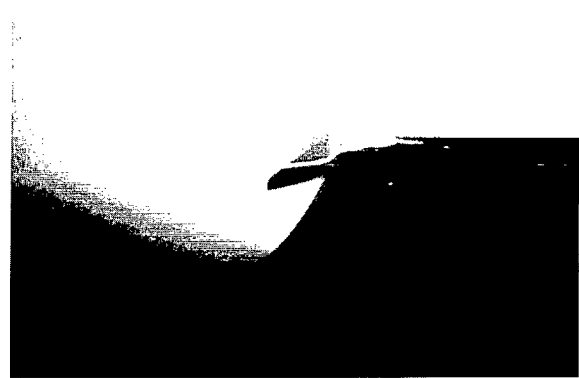
(a) $\alpha = 4^\circ$.

L-79-131

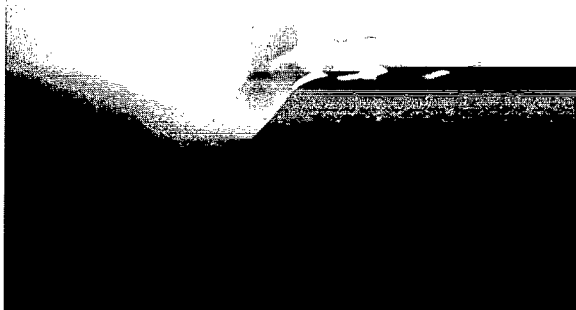
Figure 9.- Vapor-screen photographs of configuration with cambered canards at $M = 1.8$.



x = 10.16



x = 20.32



x = 30.48



x = 40.64



x = 50.80

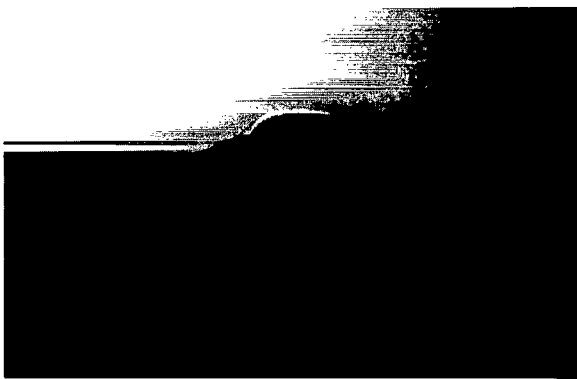


x = 60.96

(b) $\alpha = 12^\circ$.

L-79-132

Figure 9.- Concluded.



$x = 10.16$



$x = 20.32$



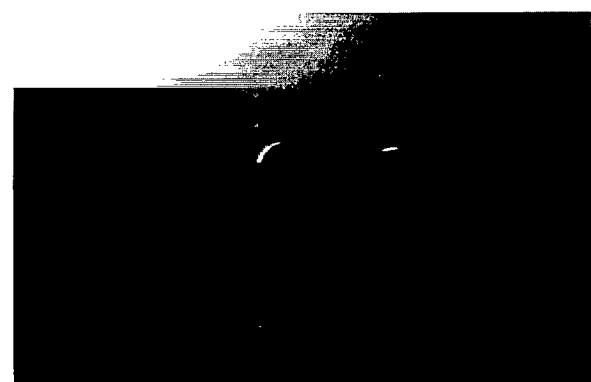
$x = 30.48$



$x = 40.64$



$x = 50.80$



$x = 60.96$

(a) $\alpha = 4^\circ$.

L-79-133

Figure 10.- Vapor-screen photographs of configuration with flat canards at $M = 1.8$.



$x = 10.16$



$x = 20.32$



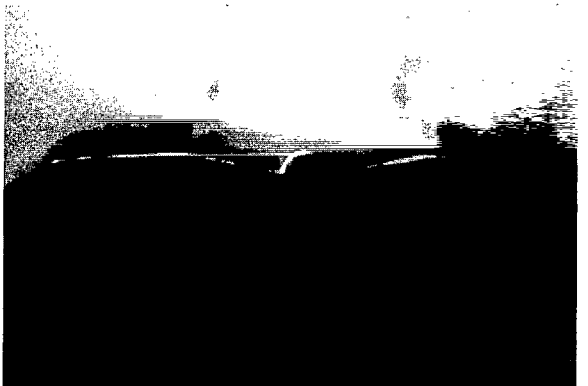
$x = 30.48$



$x = 40.64$



$x = 50.80$

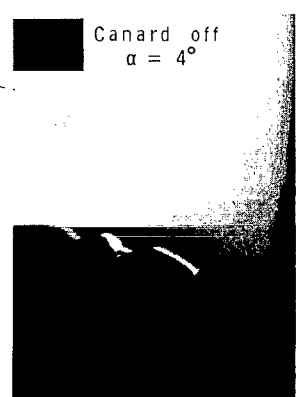
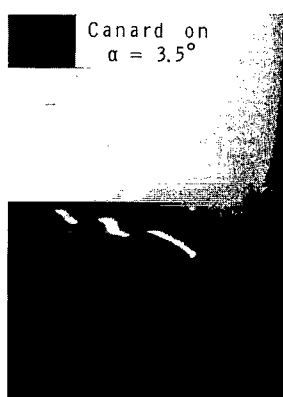
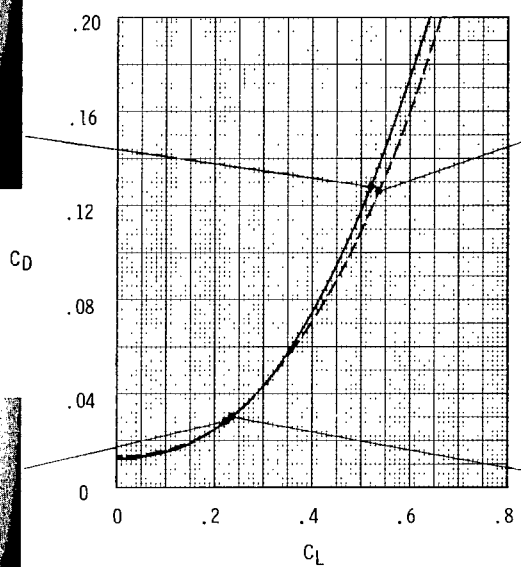
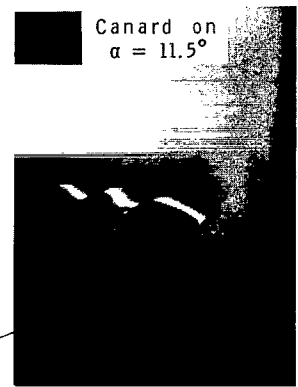


$x = 60.96$

(b) $\alpha = 12^\circ$.

L-79-134

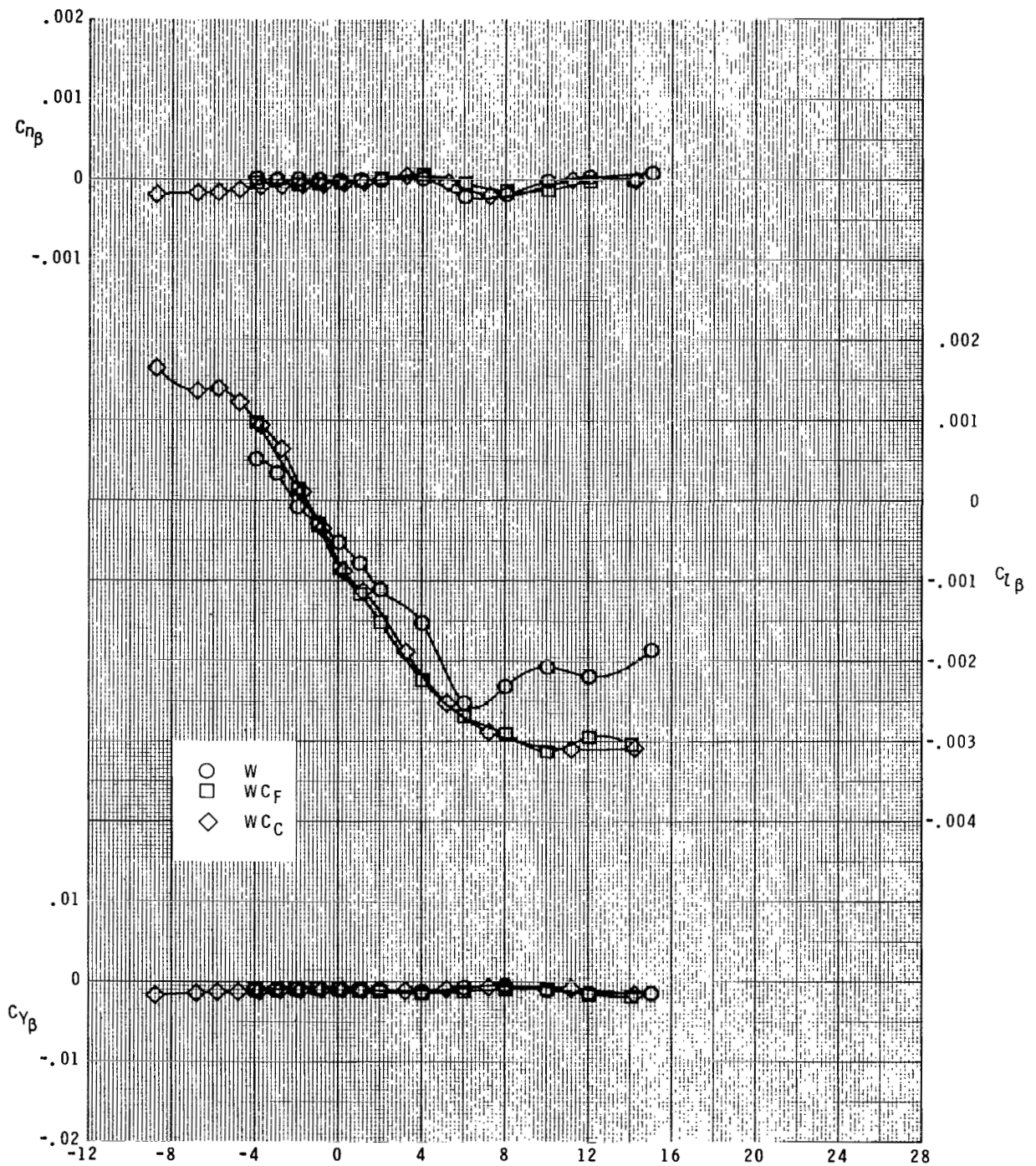
Figure 10.- Concluded.



L-79-135

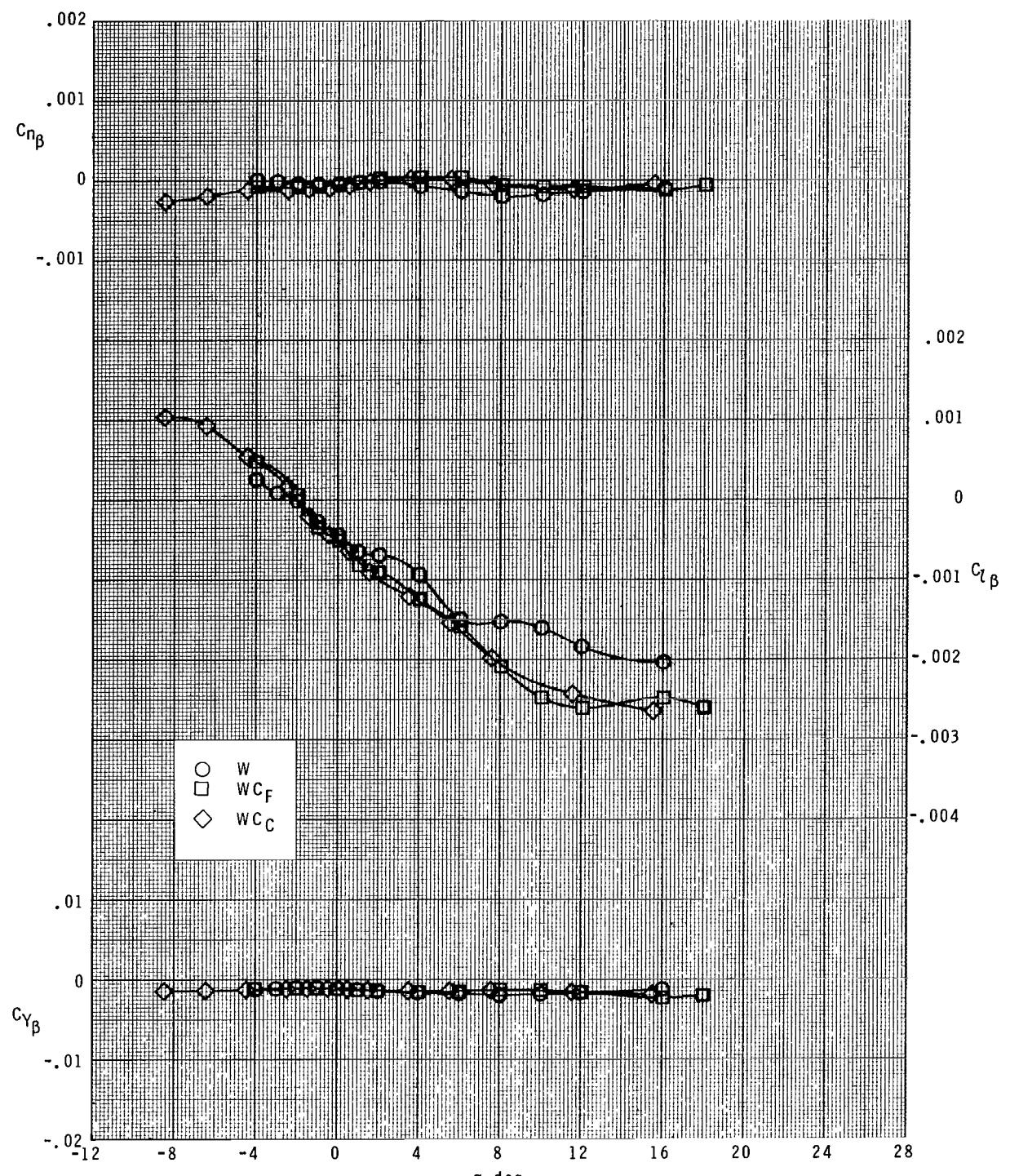
Figure 11.- Comparisons of canard-off and canard-on flow fields and drag at $M = 1.8$.





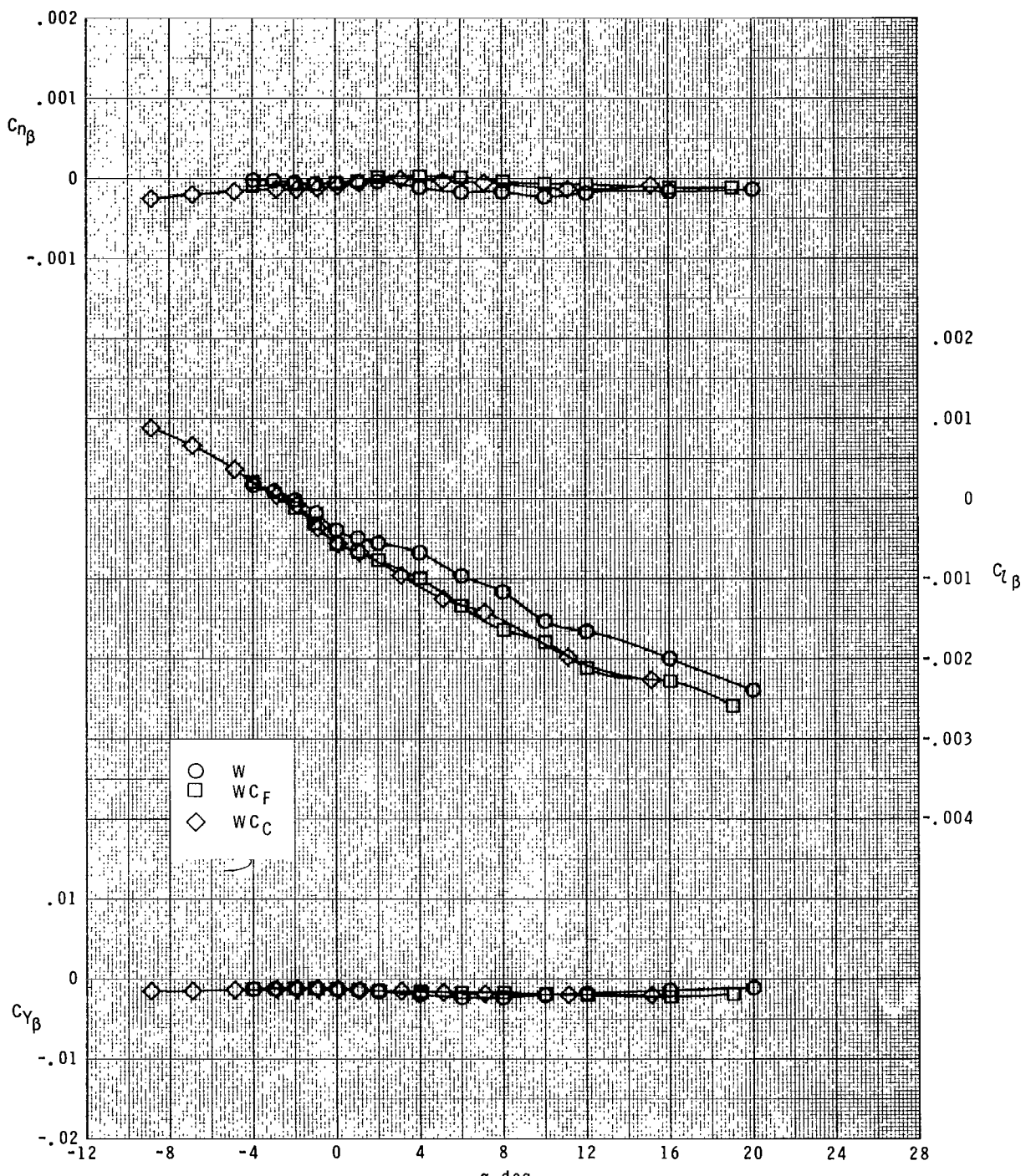
(a) $M = 1.5$.

Figure 12.- Lateral aerodynamic characteristics.



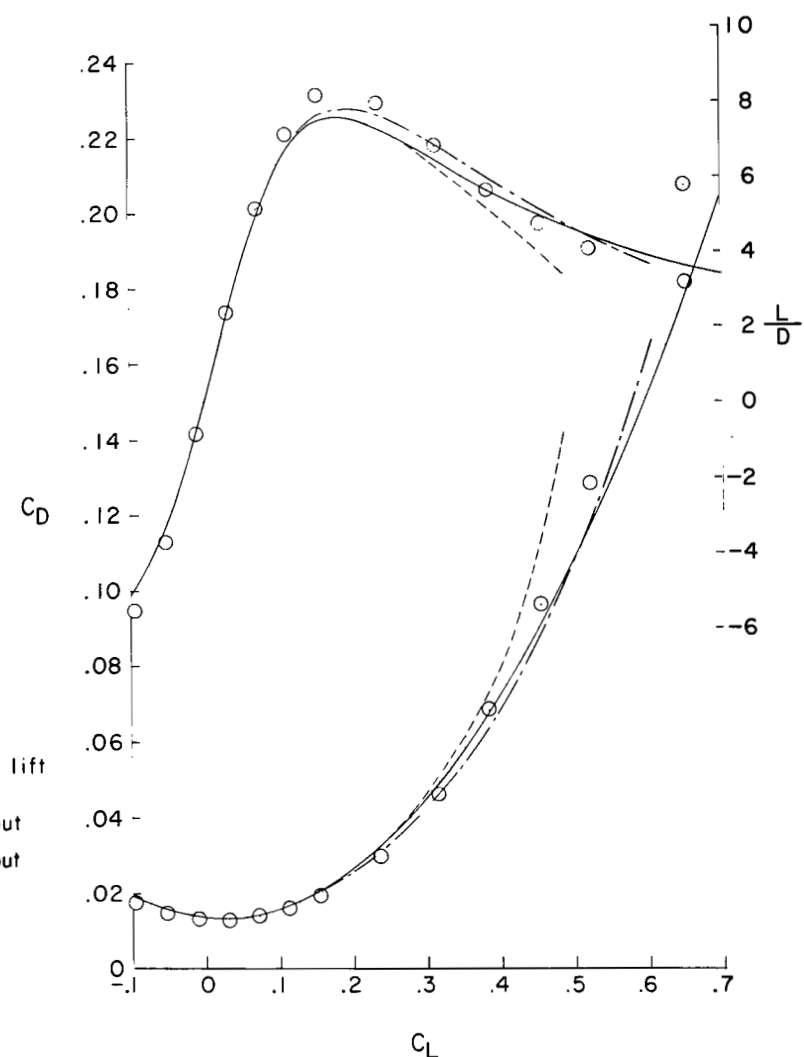
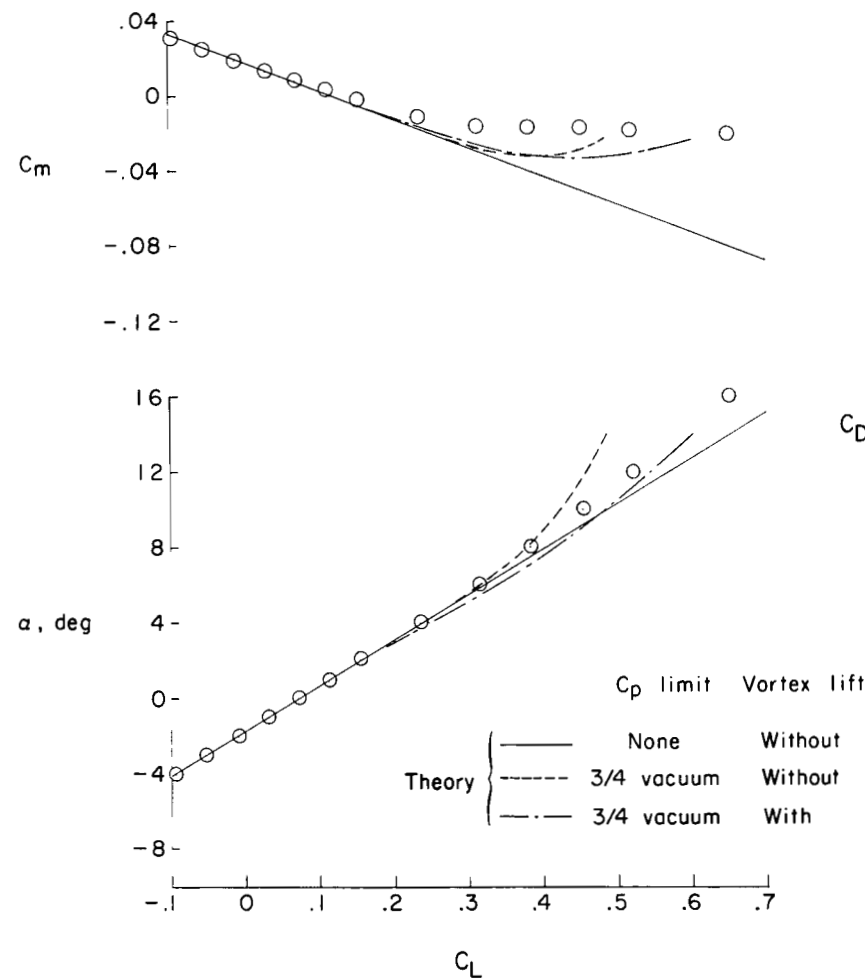
(b) $M = 1.8$.

Figure 12.- Continued.



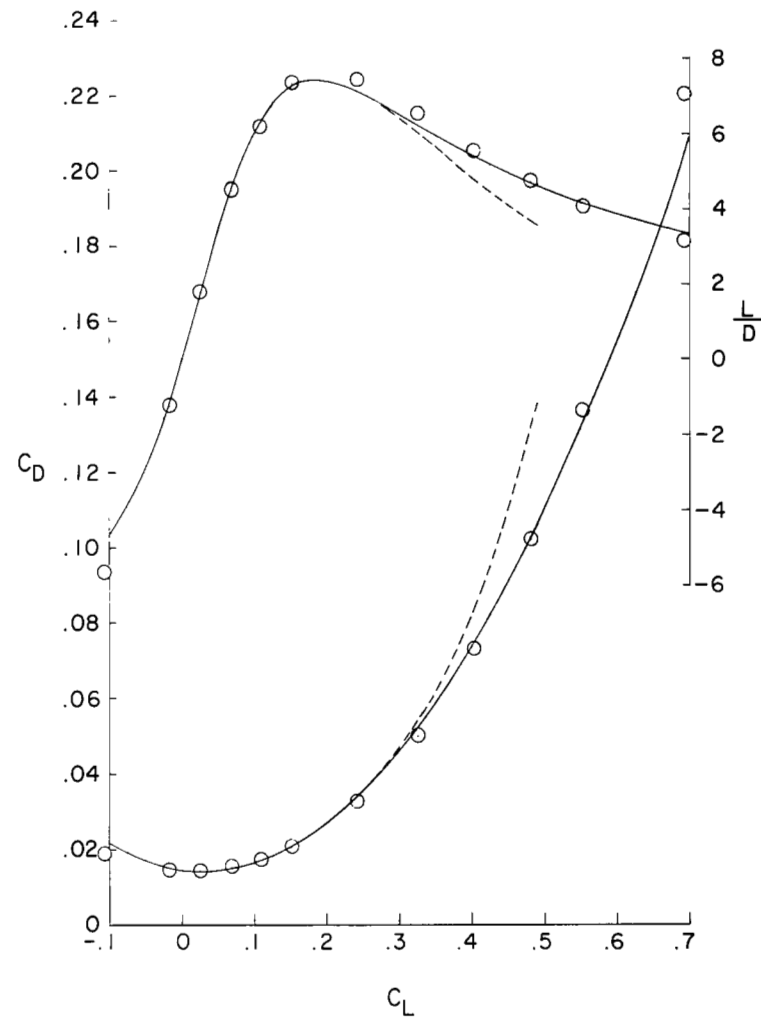
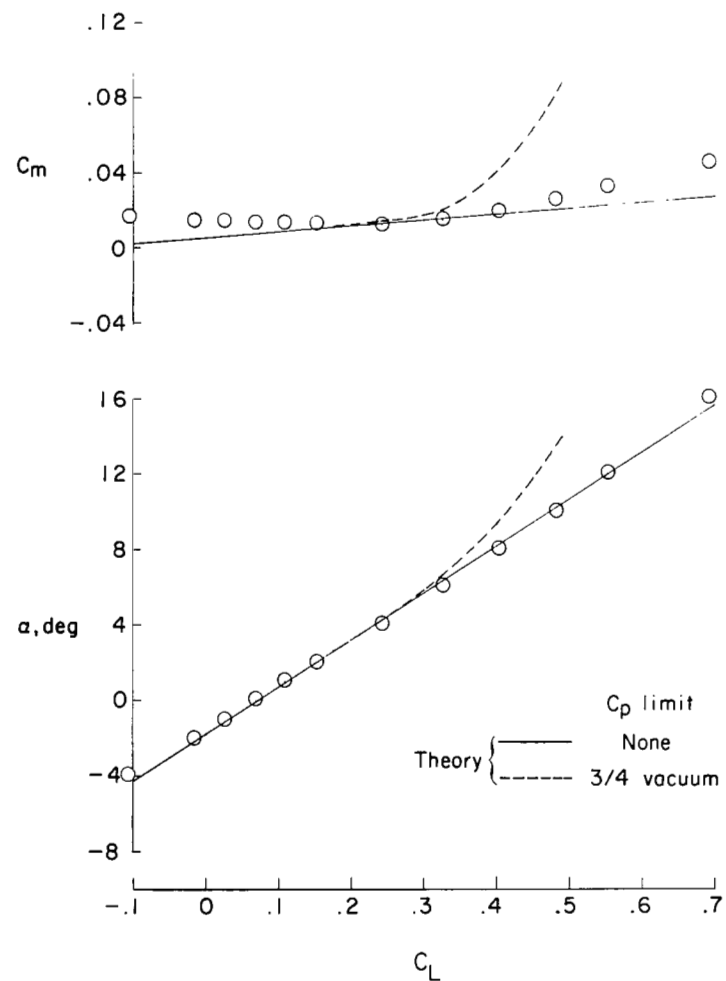
(c) $M = 2.0.$

Figure 12.- Concluded.



(a) Without canards.

Figure 13.- Experimental and theoretical comparison of longitudinal aerodynamic characteristics of the configuration at $M = 1.8$.



(b) With flat canard.

Figure 13.- Concluded.

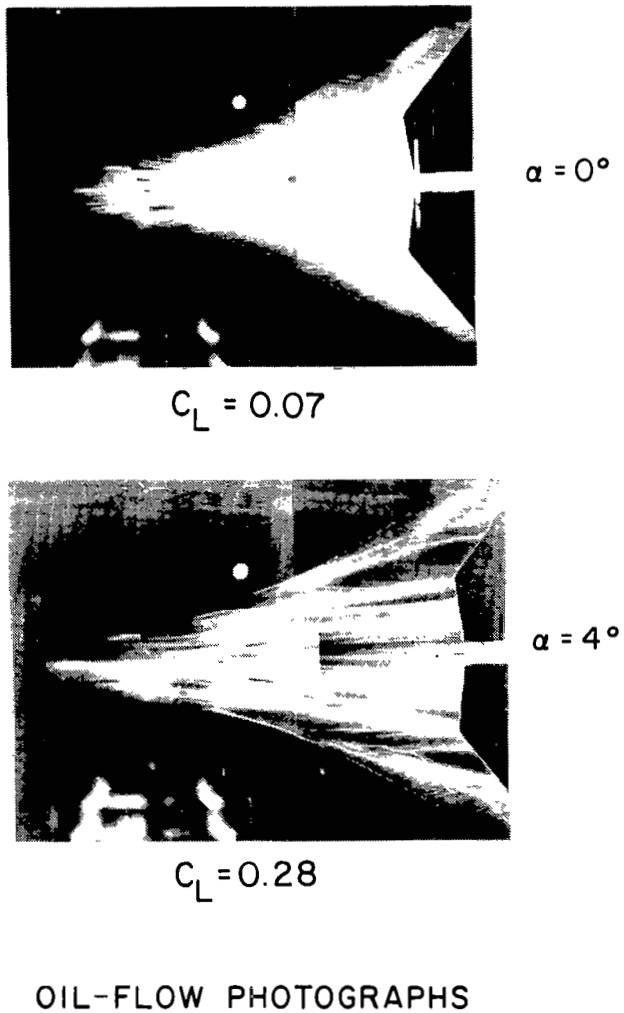
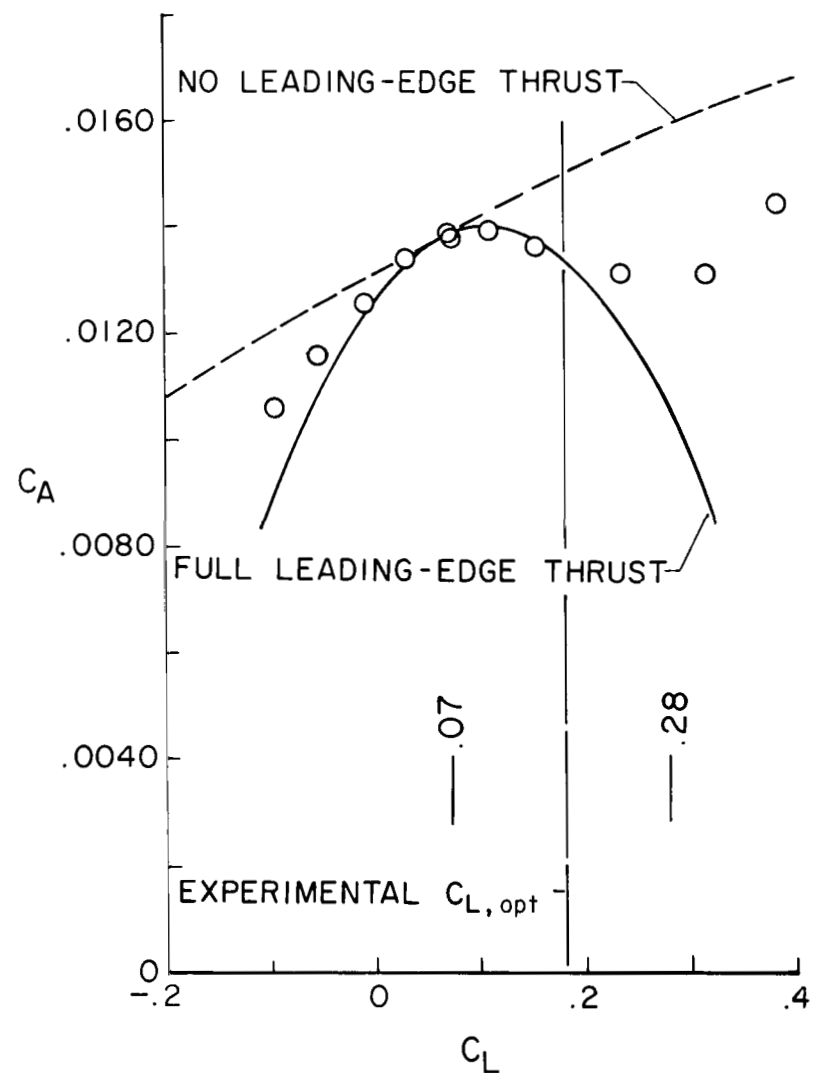


Figure 14.- Comparison of experimental and theoretical values of axial-force coefficient for the configuration without canards at $M = 1.8$.

L-79-136

1. Report No. NASA TP-1427	2. Government Accession No.	3. Recipient's Catalog No.	
4. Title and Subtitle AERODYNAMIC CHARACTERISTICS AT MACH NUMBERS OF 1.5, 1.8, and 2.0 OF A BLENDED WING-BODY CONFIGURATION WITH AND WITHOUT INTEGRAL CANARDS		5. Report Date May 1979	
7. Author(s) A. Warner Robins, Milton Lamb, and David S. Miller		6. Performing Organization Code	
9. Performing Organization Name and Address NASA Langley Research Center Hampton, VA 23665		8. Performing Organization Report No. L-12727	
12. Sponsoring Agency Name and Address National Aeronautics and Space Administration Washington, D.C. 20546		10. Work Unit No. 505-11-23-04	
15. Supplementary Notes		11. Contract or Grant No.	
		13. Type of Report and Period Covered Technical Paper	
		14. Sponsoring Agency Code	
16. Abstract An exploratory, experimental, and theoretical investigation was made of a cambered, twisted, and blended wing-body concept with and without integral canard surfaces. Theoretical calculations of the static longitudinal and lateral aerodynamic characteristics of the wing-body configurations were compared with the characteristics obtained from tests of a model in the Langley Unitary Plan wind tunnel. Mach numbers of 1.5, 1.8, and 2.0 and a Reynolds number per meter of 6.56×10^6 were used in the calculations and tests. Overall results suggest that planform selection is extremely important and that the supplemental application of new calculation techniques should provide a process for the design of supersonic wings in which spanwise distribution of upwash and leading-edge thrust might be rationally controlled and exploited.			
17. Key Words (Suggested by Author(s)) Supersonic wings Leading-edge thrust Wing design Canard		18. Distribution Statement Unclassified - Unlimited Subject Category 02	
19. Security Classif. (of this report) Unclassified	20. Security Classif. (of this page) Unclassified	21. No. of Pages 56	22. Price* \$5.25

* For sale by the National Technical Information Service, Springfield, Virginia 22161

NASA-Langley, 1979

National Aeronautics and
Space Administration

Washington, D.C.
20546

Official Business

Penalty for Private Use, \$300

THIRD-CLASS BULK RATE

Postage and Fees Paid
National Aeronautics and
Space Administration
NASA-451



4 1 1U,A, 043079 S00903DS
DEPT OF THE AIR FORCE
AF WEAPONS LABORATORY
ATTN: TECHNICAL LIBRARY (SUL)
KIRTLAND AFB NM 87117

NASA

S

POSTMASTER: If Undeliverable (Section 158
Postal Manual) Do Not Return